

# Semileptonic $B \rightarrow D^{**}$ decays in Lattice QCD : a feasibility study and first results

M Atoui<sup>b</sup>, B. Blossier<sup>a</sup>, V. Morénas<sup>b</sup>  
O. Pène<sup>a</sup>, K. Petrov<sup>c</sup>

May 9, 2022, version 1.9.1



<sup>a</sup> Laboratoire de Physique Théorique<sup>1</sup>,

CNRS et Université Paris-Sud XI, Bâtiment 210, 91405 Orsay Cedex, France

<sup>b</sup> Laboratoire de Physique Corpusculaire de Clermont-Ferrand<sup>2</sup>, Campus des Cézeaux

24 avenue des Landais, BP 80026, 63171 Aubière Cedex, France

<sup>c</sup>Inria Saclay, 1 rue Honoré d'Estienne d'Orves, Bâtiment Alan Turing,

Campus de l'Ecole Polytechnique, 91120 Palaiseau, France

## Abstract

We compute the decays  $B \rightarrow D_0^*$  and  $B \rightarrow D_2^*$  with finite masses for the  $b$  and  $c$  quarks. We first discuss the spectral properties of both the  $B$  meson as a function of its momentum and of the  $D_0^*$  and  $D_2^*$  at rest. We compute the theoretical formulae leading to the decay amplitudes from the three-point and two-point correlators. We then compute the amplitudes at zero recoil of  $B \rightarrow D_0^*$  which turn out not to be vanishing contrary to what happens in the heavy quark limit. This opens a possibility to get a better agreement with experiment, although our extrapolation to the continuum and the physical  $B$  mass has more than 100 % uncertainty. The  $B \rightarrow D_2^*$  vanishes at zero recoil and we show a statistically significant signal which is in a range between 1 to 10 times the heavy quark limit prediction. The improvement of these preliminary results will come mainly from adding a smaller lattice spacing to our sample.

LPC-Clermont RI 13-07

LPT-Orsay-13-101

<sup>1</sup>Unité Mixte de Recherche 8627 du Centre National de la Recherche Scientifique

<sup>2</sup>Unité Mixte de Recherche 6533 CNRS/IN2P3 - Université Blaise Pascal

# 1 Introduction

Understanding the composition of the final state in  $B$  meson semileptonic decay into charm meson is of key importance to control the theoretical error on the CKM matrix element  $V_{cb}$ . The discrepancy between the inclusive determination and the exclusive one, based on  $B \rightarrow D^{(*)}l\nu$ , is still of the order of  $3\sigma$  [1]. A significant part of the total width  $\Gamma(B \rightarrow X_c l \nu)$  comes from excited states: it was recently argued that the radial excitation  $D'$  might be particularly favoured, implying a suppression of the  $B \rightarrow D^*$  form factors as suggested by a study performed using the Operator Product Expansion formalism [2]. Another group of states that contribute to the width, about one quarter of it, is orbital excitations, in other words, positive parity charmed mesons, that we will note  $D^{**}$  hereafter. They are not well understood: indeed there seems to be a persistent discrepancy between claims from theory and from experiment [3], while a comparison between semileptonic decay and non leptonic decay  $B \rightarrow D^{**}\pi$ , involving the same form factors (at least in the case of the so-called Class I process), is quite confusing on the experimental side. Two types of  $D^{**}$  are observed: two “narrow resonances”  $D_{3/2}$  and a couple of “broad resonances”  $D_{1/2}$ , in the same mass region [4]. While experiments point towards a dominance of the broad resonances in semileptonic decays, theory points rather towards a dominance of the narrow resonances: not only a series of sum rules [5, 6] derived from QCD obtains that hierarchy, but also calculations with quark models [7] - [9] and lattice computations performed in the quenched approximation [10] and with  $N_f = 2$  dynamical quarks [11]. However, the main limitation of these results is that they are derived in the heavy quark limit.  $1/m_c$  corrections might be pretty large and, before getting any definitive conclusion on the disagreement between theory and experiment in that sector of flavour physics, it is mandatory to reduce the sources of systematic errors on the theory side.

## 2 Theoretical framework

In this paragraph, all the main formulae up to the differential decay rates will be given for the semileptonic decays of a  $B$  heavy meson into the first orbitally excited  $D^{**}$  mesons.

We will focus our study on the production of the  $|^3P_0\rangle$  (scalar  $D_0^*$ ) and the  $|^3P_2\rangle$  (tensor  $D_2^*$ ) states<sup>3</sup>.

Finally, we will also give relations in the case where the mass of the lepton cannot be neglected.

### 2.1 Form factors

In order to derive the decay rates, we need the transition amplitudes. They can be described using 6 form factors [12].

$^3P_2$  state :

$$\begin{aligned} \langle ^3P_2(p_{D_2^*}, \varepsilon(p_{D_2^*}, \lambda)) | V_\mu | B(p_B) \rangle &= i \boxed{\tilde{h}} \epsilon_{\mu\nu\lambda\rho} \varepsilon_{(p_{D_2^*}, \lambda)}^{*\nu\alpha} p_{B\alpha} (p_B + p_{D_2^*})^\lambda (p_B - p_{D_2^*})^\rho \\ \langle ^3P_2(p_{D_2^*}, \varepsilon(p_{D_2^*}, \lambda)) | A_\mu | B(p_B) \rangle &= \boxed{\tilde{k}} \varepsilon_{\mu\nu}^{*(p_{D_2^*}, \lambda)} p_B^\nu + \left( \varepsilon_{\alpha\beta}^{*(p_{D_2^*}, \lambda)} p_B^\alpha p_B^\beta \right) \left[ \boxed{\tilde{b}_+} (p_B + p_{D_2^*})_\mu + \boxed{\tilde{b}_-} (p_B - p_{D_2^*})_\mu \right] \end{aligned} \quad (2.1)$$

$^3P_0$  state :

$$\begin{aligned} \langle ^3P_0(p_{D_0^*}) | V_\mu | B(p_B) \rangle &= 0 \quad (\text{parity invariance}) \\ \langle ^3P_0(p_{D_0^*}) | A_\mu | B(p_B) \rangle &= \boxed{\tilde{u}_+} (p_B + p_{D_0^*})_\mu + \boxed{\tilde{u}_-} (p_B - p_{D_0^*})_\mu \end{aligned} \quad (2.2)$$

where  $V_\mu$  denotes the vector current  $\bar{c}\gamma_\mu b$  and  $A_\mu$  the axial current  $\bar{c}\gamma_\mu\gamma_5 b$ .

$\varepsilon(p_{D_2^*}, \lambda)$  is the polarisation tensor of the  $^3P_2$  state ( $\lambda$  being the projection of the  $J = 2$  total angular momentum along some quantification axis).

Moreover, the chosen normalisation of the mesonic states is

$$\langle M(p') | M(p) \rangle = (2\pi)^3 2E \delta^3(\vec{p}' - \vec{p}).$$

Finally, because of parity and time-reversal invariance of the strong interactions, those form factors are real numbers.

<sup>3</sup>We use the  $|^{2S+1}L_J\rangle$  notation of the states, where  $S$  is the spin angular momentum,  $L = 1$  the orbital angular momentum and  $J = L + S$  the total angular momentum of the  $D^{**}$  state.

## 2.2 Differential decay rates

The goal is to compute the differential decay width  $d\Gamma(\bar{B} \rightarrow D^{**} \ell \bar{\nu})$  whose general expression is

$$d\Gamma(\bar{B} \rightarrow D^{**} \ell \bar{\nu}) = \frac{1}{2 E_B} |\bar{\mathcal{M}}|^2 d\Phi,$$

$$\text{with } \begin{cases} d\Phi = \frac{d^3 \vec{p}_{D^{**}}}{(2\pi)^3 2E_{D^{**}}} \frac{d^3 \vec{p}_\ell}{(2\pi)^3 2E_\ell} \frac{d^3 \vec{p}_\nu}{(2\pi)^3 2E_\nu} (2\pi)^4 \delta^{(4)}(p_B - p_{D^{**}} - p_\ell - p_\nu), \\ |\bar{\mathcal{M}}|^2 = \sum_{\mu, \nu} W_{\mu\nu} \ell^{\mu\nu}. \end{cases}$$

In the last equality,  $W_{\mu\nu}$  denotes the hadronic tensor

$$W_{\mu\nu}(p_B, p_{D^{**}}) = \frac{G_F^2 |V_{cb}|^2}{2} \sum_{\text{final spins}} \langle D^{**}(p_{D^{**}}) | V_\mu - A_\mu | \bar{B}(p_B) \rangle \langle \bar{B}(p_B) | V_\nu - A_\nu | D^{**}(p_{D^{**}}) \rangle,$$

where the transition amplitudes have been given in the preceding paragraph (let us note that there are no summation nor average over the initial spins since the  $\bar{B}$  meson has a spin equal to zero) and  $\ell^{\mu\nu}$  represents the leptonic tensor

$$\ell^{\mu\nu}(p_\ell, p_\nu) = \sum_s [\bar{u}_\ell(p_\ell, s) \gamma^\mu (1 - \gamma^5) v_\nu(p_\nu)] [\bar{u}_\ell(p_\ell, s) \gamma^\nu (1 - \gamma^5) v_\nu(p_\nu)]^*$$

In that last formula,  $u_\ell(p_\ell, s)$  is the lepton  $\ell$  spinor ( $s$  denotes the usual projection of its spin), while  $v_\nu(p_\nu)$  represents the antineutrino  $\bar{\nu}$  spinor.

All that remains is to compute the leptonic tensor, then the hadronic tensor and the measure  $d\Phi$  of the phase space in order to obtain the expressions of the differential decay widths.

### 2.2.1 Leptonic tensor $\ell^{\mu\nu}$

The calculation is classical and straightforward, leading to

$$\ell^{\mu\nu} = 8 [p_\ell^\mu p_\nu^\nu + p_\ell^\nu p_\nu^\mu - (p_\ell \cdot p_\nu) g^{\mu\nu} - i \epsilon^{\mu\nu\rho\sigma} (p_\ell)_\rho (p_\nu)_\sigma].$$

We can notice that the mass of the lepton has vanished, which renders the expression valid in the situations where  $m_\ell = 0$  as well as  $m_\ell \neq 0$ .

### 2.2.2 Hadronic tensor $W_{\mu\nu}$

By looking at the expressions of the transition amplitudes given above, the general structure of the hadronic tensor can be inferred and put into the form [12]:

$$W_{\mu\nu} = \frac{G_F^2 |V_{cb}|^2}{2} \left[ \boxed{\alpha} g_{\mu\nu} + \boxed{\beta_{++}} (p_B + p_{D^{**}})_\mu (p_B + p_{D^{**}})_\nu + \boxed{\beta_{+-}} (p_B + p_{D^{**}})_\mu (p_B - p_{D^{**}})_\nu \right. \\ \left. + \boxed{\beta_{-+}} (p_B - p_{D^{**}})_\mu (p_B + p_{D^{**}})_\nu + \boxed{\beta_{--}} (p_B - p_{D^{**}})_\mu (p_B - p_{D^{**}})_\nu + i \boxed{\gamma} \epsilon_{\mu\nu\rho\sigma} (p_B + p_{D^{**}})^\rho (p_B - p_{D^{**}})^\sigma \right]. \quad (2.3)$$

The coefficients  $\alpha, \beta_{++}, \beta_{+-}, \beta_{-+}, \beta_{--}$  and  $\gamma$  are given in the Appendix for the  $^3P_0$  and the  $^3P_2$  states.

### 2.2.3 Kinematics and notations

For reasons of simplification, we now choose to compute the decay rates in the rest frame of the  $\bar{B}$  meson.

We then define two dimensionless parameters  $x$  and  $y$  according to

$$\boxed{x m_B = 2 E_\ell} \quad \text{as well as} \quad \boxed{y m_B^2 = (p_B - p_{D^{**}})^2 = (p_\ell + p_\nu)^2}$$

where  $E_\ell$  is the energy of the lepton in the  $\bar{B}$  rest frame.

We introduce also the mass ratio  $r_X$

$$\boxed{m_X = r_X m_B} \quad \text{where } X \text{ is either a } D^{**} \text{ meson or the lepton } \ell$$

Many kinematical terms can be expressed with these three parameters, such as

$$E_{D^{**}} = \frac{m_B}{2} (1 - y + r_{D^{**}}^2) \quad ; \quad p_\ell \cdot p_\nu = \frac{1}{2} m_B^2 (y - r_\ell^2) \quad ; \quad p_\ell \cdot p_{D^{**}} = \frac{1}{2} m_B^2 (x - y - r_\ell^2) \quad ; \quad p_B \cdot p_\ell = \frac{1}{2} m_B^2 x \quad .$$

### 2.2.4 Measure $d\Phi$ of the phase space

The goal is to get the differential widths  $d\Gamma$  with respect to the lepton energy  $E_\ell$  and the momentum transfer  $(p_B - p_{D^{**}})^2$ , in other words with respect to the variables  $x$  and  $y$  :  $d^2\Gamma/dx dy$

So we must integrate over the antineutrino momentum  $\vec{p}_\nu$ , then over all possible orientations of  $\vec{p}_\ell$  so that only the dependance on  $E_\ell$  (i.e. on  $x$ ) remains, and finally over all possible directions of the 3-vector  $\vec{p}_{D^{**}}$  since we want to keep the dependance on  $E_{D^{**}}$  (i.e. on  $y$ ). We finally get :

$$d\Phi = -\frac{m_B^2}{128\pi^3} dx dy \theta(1 - x + y - r_{D^{**}}^2).$$

### 2.2.5 Constraints on $x$ and $y$

The parameters  $x$  and  $y$ , that is the lepton energy ( $E_\ell$ ) and the  $D^{**}$  meson energy ( $E_{D^{**}}$ ), cannot be arbitrary. They are constrained by two conditions : one which is obvious in the expression of  $d\Phi$  above (the Heaviside function) and another one which appeared during the integration over the direction of  $\vec{p}_\ell$ . In other terms, we have access to the variation domains of both parameters  $x$  and  $y$  whether we consider  $x = x(y)$  or  $y = y(x)$ : they are given in the Appendix.

### 2.2.6 Differential decay widths in the $\bar{B}$ rest frame

Using the definition of  $d\Gamma$  as well as all the preceding results, the construction of the differential decay widths proceeds in the following way :

$$\frac{d\Gamma}{dx dy}(\bar{B} \rightarrow D^{**} \ell \bar{\nu}) = -\frac{m_B}{256\pi^3} |\mathcal{M}|^2$$

where  $|\mathcal{M}|^2 = W_{\mu\nu} \ell^{\mu\nu}$  becomes in this particular frame

$$\begin{aligned} |\mathcal{M}|^2 = 2 G_F^2 |V_{cb}|^2 m_B^2 & \left\{ -2[\alpha](y - r_\ell^2) \right. \\ & - [\beta_{++}] m_B^2 \left[ 4[x r_{D^{**}}^2 + (1-x)(y-x)] + r_\ell^2 [3y - 4(x + r_{D^{**}}^2) + r_\ell^2] \right] \\ & + \left( [\beta_{+-}] + [\beta_{-+}] \right) m_B^2 r_\ell^2 \left[ 2(1-x - r_{D^{**}}^2) + y + r_\ell^2 \right] \\ & + [\beta_{--}] m_B^2 r_\ell^2 (y - r_\ell^2) \\ & \left. - 2[\gamma] m_B^2 \left[ y(1+y-2x-r_{D^{**}}^2) + r_\ell^2(1+y-r_{D^{**}}^2) \right] \right\} \end{aligned}$$

We can notice that, for a zero mass lepton, only the coefficients  $\alpha$ ,  $\beta_{++}$  and  $\gamma$  survive.

The expressions for each  $D^{**}$  are also written in the Appendix. However, their use requires the knowledge of the momentum dependance of the form factors. In the following, we will focus on a method to obtain such a dependance.

## 2.3 Extracting the form factors from the transition amplitudes

On the lattice, we compute the transition amplitudes for different momenta of the mesons. But we need the momentum dependance of the form factors in order to calculate the decay rates of the semileptonic decays of the  $B$  to a  $D^{**}$ . So we must devise a way to extract the form factors from the lattice transition amplitudes.

### 2.3.1 Kinematics

We will work in the rest frame of the  $D^{**}$  meson<sup>4</sup> and the  $B$  meson will carry the momentum. Moreover, we will work with  $B$ 's whose spatial momentum is symmetrical.

$$p_{D^{**}} = (m_{D^{**}}, \vec{0}) \quad \text{and} \quad p_B^\mu = (E_B, p, p, p) \quad .$$

We will choose the Minkowski metrics:  $g_{\mu\nu} = \text{Diag}(+, -, -, -)$

---

<sup>4</sup>This will greatly simplify the calculations on the lattice.

The other piece we need is the expression of the polarisation tensor for the  ${}^3P_2$  state in the  $D^{**}$  rest frame, that is  $\varepsilon(\vec{0}, \lambda)$ . We can construct it from the combination of two spin-1 states

$$\varepsilon^{\mu\nu}(\vec{0}, \lambda) = \sum_{s, s'} \langle 1 \ 1 \ s \ s' | 2 \ \lambda \rangle \varepsilon^\mu(\vec{0}, s) \varepsilon^\nu(\vec{0}, s'),$$

where the Clebsch-Gordan coefficients for  $1 + 1 \rightarrow 2$  appear, as well as the polarisation vector  $\varepsilon^\mu(\vec{0}, s)$  of a spin-1 state. The final expressions are gathered in the Appendix.

### 2.3.2 ${}^3P_0$ form factors

Using the notation

$$\mathcal{T}_\mu^A \stackrel{\text{def.}}{=} \langle {}^3P_0 | A_\mu | B(p_B) \rangle,$$

we explicitly get from Eqs. (2.2):

$$\begin{cases} \mathcal{T}_0^A = \boxed{\tilde{u}_+}(E_B + m_{D^{**}}) + \boxed{\tilde{u}_-}(E_B - m_{D^{**}}) & \text{(temporal direction),} \\ \mathcal{T}_i^A = \boxed{\tilde{u}_+}p + \boxed{\tilde{u}_-}p & \text{(spatial direction).} \end{cases}$$

So it is straightforward to express  $\tilde{u}_+$  and  $\tilde{u}_-$  with the  $\mathcal{T}_\mu^A$ 's. The results are presented in the Appendix.

### 2.3.3 ${}^3P_2$ form factors

In the following, we will adopt the notation:

$$\mathcal{T}_{\mu(\lambda)}^A \stackrel{\text{def.}}{=} \langle {}^3P_2(\lambda) | A_\mu | B(p_B) \rangle \quad \text{as well as} \quad \mathcal{T}_{\mu(\lambda)}^V \stackrel{\text{def.}}{=} \langle {}^3P_2(\lambda) | V_\mu | B(p_B) \rangle.$$

In order to extract one particular form factor, we can choose in Eqs. (2.1) either some spatial direction where each coefficient of the other form factors vanishes, or we can construct a linear combination of the  $\mathcal{T}_{i(\lambda)}^A$  and/or the  $\mathcal{T}_{i(\lambda)}^V$ . This procedure can be carried out by using the expressions for the polarisation tensor and the four-momenta at our disposal and calculating the contribution of the corresponding terms appearing in the matrix elements (2.1) which define the form factors (those contributions are gathered in Table 1).

A few possibilities are collected in the Appendix.

## 2.4 Summary

We have constructed all the theoretical formulae which allow us to calculate the decay widths of the semileptonic  $B \rightarrow D^{**}$  channels. The strategy to use them is the following :

1. compute, on the lattice, the transition amplitudes for the  $B \rightarrow D^{**}$  processes.
2. extract the form factors from them.
3. use the formulae in the Appendix to obtain the decay widths.

We expect the lattice  ${}^3P_2$  computation to be somewhat tricky so we are going to estimate first the contribution of the  $\tilde{k}$ ,  $\tilde{b}_+$ ,  $\tilde{b}_-$  and  $\tilde{h}$  form factors to the  $\bar{B} \rightarrow D_2^* \ell \bar{\nu}$  decay width.

## 2.5 Estimation of the contribution of the form factors to the ${}^3P_2$ decay width

There are 4 form factors needed to describe the transition amplitudes from a  $B$  to a  ${}^3P_2$  state which increases the difficulty in the lattice computations. So it could be useful to have an idea of each of their contribution to the decay widths. In order to get a quantitative hint, we will relate these form factors to their infinite mass limit  $\tau_{3/2}$  and use this  $\tau_{3/2}$  to produce a numerical estimation.

$\varepsilon_{\mu\nu}^{(\lambda)}$	$\varepsilon_{\mu\nu}^{(\lambda)} p_B^\nu$	$\varepsilon_{(\lambda)}^{\mu\nu}$	$\varepsilon_{(\lambda)}^{\mu\nu} p_{B\nu}$
$\varepsilon_{\mu\nu}^{(+2)}$	$\frac{p}{2} (0, 1+i, i-1, 0)$	$\varepsilon_{(+2)}^{\mu\nu}$	$-\frac{p}{2} (0, 1+i, -1+i, 0)$
$\varepsilon_{\mu\nu}^{(+1)}$	$-\frac{p}{2} (0, 1, i, 1+i)$	$\varepsilon_{(+1)}^{\mu\nu}$	$\frac{p}{2} (0, 1, i, 1+i)$
$\varepsilon_{\mu\nu}^{(0)}$	$-\frac{p}{\sqrt{6}} (0, 1, 1, -2)$	$\varepsilon_{(0)}^{\mu\nu}$	$\frac{p}{\sqrt{6}} (0, 1, 1, -2)$
$\varepsilon_{\mu\nu}^{(-1)}$	$\frac{p}{2} (0, 1, -i, 1-i)$	$\varepsilon_{(-1)}^{\mu\nu}$	$\frac{p}{2} (0, -1, i, -1+i)$
$\varepsilon_{\mu\nu}^{(-2)}$	$\frac{p}{2} (0, 1-i, -1-i, 0)$	$\varepsilon_{(-2)}^{\mu\nu}$	$\frac{p}{2} (0, -1+i, 1+i, 0)$
$\varepsilon_{\mu\nu}^{(+2)} + \varepsilon_{\mu\nu}^{(-2)}$	$p (0, 1, -1, 0)$	$\varepsilon_{(+2)}^{\mu\nu} + \varepsilon_{(-2)}^{\mu\nu}$	$p (0, -1, 1, 0)$
$\varepsilon_{\mu\nu}^{(+2)} - \varepsilon_{\mu\nu}^{(-2)}$	$p (0, i, i, 0)$	$\varepsilon_{(+2)}^{\mu\nu} - \varepsilon_{(-2)}^{\mu\nu}$	$p (0, -i, -i, 0)$
$\varepsilon_{\mu\nu}^{(+1)} + \varepsilon_{\mu\nu}^{(-1)}$	$p (0, 0, -i, -i)$	$\varepsilon_{(+1)}^{\mu\nu} + \varepsilon_{(-1)}^{\mu\nu}$	$p (0, 0, i, i)$
$\varepsilon_{\mu\nu}^{(+1)} - \varepsilon_{\mu\nu}^{(-1)}$	$p (0, -1, 0, -1)$	$\varepsilon_{(+1)}^{\mu\nu} - \varepsilon_{(-1)}^{\mu\nu}$	$p (0, 1, 0, 1)$

$\varepsilon_{(\lambda)}^{\mu\nu}$	$\varepsilon_{(\lambda)}^{\mu\nu} p_{B\mu} p_{B\nu}$
$\varepsilon_{(+2)}^{\mu\nu}$	$i p^2$
$\varepsilon_{(+1)}^{\mu\nu}$	$-(1+i) p^2$
$\varepsilon_{(0)}^{\mu\nu}$	$0$
$\varepsilon_{(-1)}^{\mu\nu}$	$(1-i) p^2$
$\varepsilon_{(-2)}^{\mu\nu}$	$-i p^2$
$\varepsilon_{(+2)}^{\mu\nu} + \varepsilon_{(-2)}^{\mu\nu}$	$0$
$\varepsilon_{(+2)}^{\mu\nu} - \varepsilon_{(-2)}^{\mu\nu}$	$2i p^2$
$\varepsilon_{(+1)}^{\mu\nu} + \varepsilon_{(-1)}^{\mu\nu}$	$-2i p^2$
$\varepsilon_{(+1)}^{\mu\nu} - \varepsilon_{(-1)}^{\mu\nu}$	$-2 p^2$

Table 1: Contributions of the polarisation tensor in the  $B \rightarrow {}^3P_2$  transition amplitude

### 2.5.1 Infinite mass limit

In the limit where the heavy quark of the meson has an infinite mass, new symmetries (and thus additional conserved quantities) appear. These new symmetries provide additional relations between the transition amplitudes so that the form factors become dependant. It can be proven [13] that this reduction of the form factors leads to the following relations for the  ${}^3P_2$  state :

$$\left\{ \begin{array}{l} \tilde{h} = \frac{\sqrt{3}}{2} \frac{1}{m_B^2 \sqrt{r_{D_2^*}}} \tau_{3/2} \\ \tilde{b}_+ = -\frac{\sqrt{3}}{2} \frac{1}{m_B^2 \sqrt{r_{D_2^*}}} \tau_{3/2} \end{array} \right. \quad \left\{ \begin{array}{l} \tilde{k} = \sqrt{3} \sqrt{r_{D_2^*}} (1+w) \tau_{3/2} \\ \tilde{b}_- = \frac{\sqrt{3}}{2} \frac{1}{m_B^2 \sqrt{r_{D_2^*}}} \tau_{3/2} \end{array} \right.$$

where the parameter  $w$  is defined by :

$$m_B m_{D_2^*} w = p_B \cdot p_{D_2^*} \quad \Longrightarrow \quad \boxed{y = 1 + r_{D^{**}}^2 - 2 r_{D^{**}} w}$$

and  $\tau_{3/2}$  is one of the so-called Isgur-Wise functions.

### 2.5.2 Fit of $\tau_{3/2}$

Using a covariant construction of the transition amplitudes in the infinite mass limit (quark models à la Bakamjian-Thomas), it has been shown [7] that the Isgur-Wise function  $\tau_{3/2}$  can be well fitted by :

$$\tau_{3/2}(w) = \tau_{3/2}(1) \left( \frac{2}{1+w} \right)^{2\sigma_{3/2}^2} \implies \tau_{3/2}(y) = \tau_{3/2}(1) \left[ \frac{4r_{D_2^*}}{(1+r_{D_2^*})^2 - y} \right]^{2\sigma_{3/2}^2}$$

where the accessible phase space domain is given by :

$$1 \leq w \leq \frac{m_B^2 + m_{D^{**}}^2}{2m_B m_{D^{**}}} \implies (1 - r_{D_2^*})^2 \geq y \geq 0$$

We will also take (GI model in [7]) :  $\tau_{3/2}(1) \simeq 0.539$  as well as  $\sigma_{3/2}^2 \simeq 1.50$ .

### 2.5.3 Quantitative prediction of each contribution to the total width

We are now in position to estimate the contribution of each form factor to the total width of the  $\bar{B} \rightarrow D_2^* \ell \bar{\nu}$  decay channel. Let us take the case of a zero mass lepton to simplify the calculations. Starting from the expression of  $\frac{d^2\Gamma}{dx dy}$  and with the notations given in the Appendix, we can perform both the integrations over  $x$  and  $y$  and we get :

$C_i$	$C_1 \times \tilde{k}^2$	$C_2 \times \tilde{h}^2$	$C_3 \times \tilde{b}_+^2$	$C_5 \times 2\tilde{k}\tilde{b}_+$	$C_8$
$\iint C_i \times \mathbf{FF}^2$	-61.3	-0.86	-4.43	29.0	0

We can notice that the biggest contributions come from the terms where the  $\tilde{k}$  form factor appears; that is why we will focus on its determination in the actual lattice computation.

## 3 Simulation set up

In our analysis we use gauge ensembles produced by European Twisted Mass Collaboration [14] - [16] with  $N_f = 2$  twisted-mass fermions tuned at maximal twist. Parameters of the simulations are collected in Table 2. The gauge action is tree-level Symanzik improved [19] and reads

$$S_G[U] = \frac{\beta}{6} \left( b_0 \sum_{x, \mu \neq \nu} \text{Tr} \left( 1 - P^{1 \times 1}(x; \mu, \nu) \right) + b_1 \sum_{x, \mu \neq \nu} \text{Tr} \left( 1 - P^{1 \times 2}(x; \mu, \nu) \right) \right),$$

where  $b_0 = 1 - 8b_1$  and  $b_1 = -1/12$ . The fermionic action with two degenerate flavors is Wilson-like with a twisted mass term and reads [20] - [22]:

$$S_F[\chi_q, \bar{\chi}_q, U] = a^4 \sum_x \bar{\chi}_q(x) \left( D_W + i\mu_q \gamma_5 \tau_3 \right) \chi_q(x),$$

where  $D_W$  is the massless Wilson-Dirac operator. In the valence sector we add two doublets of charm quarks and “bottom” quarks. Moreover, as we are interested in computing form factors at different momenta we implement  $\theta$ -boundary conditions [23], using  $\vec{\theta} \equiv (\theta, \theta, \theta)$ , for the  $b$  doublet:

$$\chi_b(x + L\hat{e}_i) = e^{i\theta L} \chi_b(x)$$

This is equivalent to define an auxiliary field

$$\chi_b^{\vec{\theta}}(x) = e^{-i\vec{\theta} \cdot \vec{x}} \chi_b(x)$$

and a Dirac operator

$$D^{\vec{\theta}}(\chi_b, \bar{\chi}_b, U) \equiv D(\chi_b^{\vec{\theta}}, \bar{\chi}_b^{\vec{\theta}}, U^{\vec{\theta}}) \quad \text{with} \quad U_i^{\vec{\theta}}(x) = e^{ia\theta} U_i(x).$$

The whole fermionic action reads finally :

$$S^{\text{val}} = S_F[\chi_q, \bar{\chi}_q, U] + S_F[\chi_c, \bar{\chi}_c, U] + S_F[\chi_b^{\vec{\theta}}, \bar{\chi}_b^{\vec{\theta}}, U^{\vec{\theta}}].$$

We use all to all propagators with stochastic sources  $\eta[i]$  diluted in time [24] and improve the variance to signal ratio with the one-end trick [25, 26]. When it is generalised to  $\theta$ -boundary conditions, it consists in solving the Dirac equations

$$\sum_y D[f, r, \vec{\theta}]_{\alpha\beta}^{ab}(x, y) \phi[i, f, r, \vec{\theta}, \tilde{\alpha}, \tilde{t}]_{\beta}^b(y) = \eta[i]_{\alpha}^a(x) \delta_{\alpha\tilde{\alpha}} \delta_{t_x\tilde{t}},$$

$\beta$	$L^3 \times T$	$a[\text{fm}]$	# cnfgs	$\mu_{\text{sea}} = \mu_l$	$\mu_c$	$\mu_b$	$\theta [\pi/L]$
3.9	$24^3 \times 48$	0.085(3)	240	0.0085	0.215	0.3498	0.0, 0.99, 1.41 2.02, 2.50, 2.92 3.66
						0.4839	0.0, 1.21, 1.72 2.46, 3.05, 3.56 4.46
						0.6694	0.0, 1.48, 2.11 3.01, 3.73, 4.36 5.46
4.05	$32^3 \times 64$	0.069(2)	160	0.006	0.1849	0.3008	0.0, 1.09, 1.56 2.23, 2.76, 3.23 4.04
						0.4162	0.0, 1.35, 1.92 2.74, 3.40, 3.97 4.97
						0.5757	0.0, 1.67, 2.37 3.39, 4.21, 4.91 6.15

Table 2: *Parameters of the simulations used in this work; masses and momenta are expressed in lattice units. The lattice spacing  $a_{\beta=3.9}$  is fixed by imposing the matching of  $f_\pi$  obtained on the lattice to the experimental value [17] and  $a_{\beta=4.05}$  is rescaled using the parameter  $\Lambda_{\overline{\text{MS}}}^{N_f=2}$  [18].*

where  $\tau^3 \chi = r \chi$ ,  $f$  represents the fermion flavour, and

$$\sum_y D[f_2, r_2, \vec{\theta}_2]_{\alpha\beta}^{ab}(x, y) \Phi[i, f_2, r_2, f_1, r_1, \Gamma_2, \vec{\theta}_2, \vec{\theta}_1, \tilde{\alpha}, \tilde{t}, \tilde{t} + t_S]_{\beta}^b(y) = \Gamma_{2\alpha\beta} \phi[i, f_1, r_1, \vec{\theta}_1, \tilde{\alpha}, \tilde{t}]_{\beta}^a(x) \delta_{t_S, t_x - \tilde{t}}.$$

The stochastic source

$$\xi[i, \tilde{\alpha}, \tilde{t}]_{\alpha}^a(x) \equiv \eta[i]_{\alpha}^a(x) \delta_{\alpha\tilde{\alpha}} \delta_{t_x \tilde{t}}$$

is diluted in spinor and is non zero in a single time-slice  $\tilde{t}$ . It is normalized by

$$\lim_{N \rightarrow \infty} \frac{1}{N} \sum_{i=1}^N \xi[i, \tilde{\alpha}, \tilde{t}]_{\alpha}^a(x) \xi^*[i, \tilde{\alpha}, \tilde{t}]_{\beta}^b(y) = \delta_{ab} \delta_{\alpha\beta} \delta_{xy} \delta_{\alpha\tilde{\alpha}} \delta_{t_x \tilde{t}}.$$

In order to improve the overlap of the interpolating fields for the ground states or to create operator of higher spin (for instance the tensor meson  $D_2^*$ ), one has to use interpolating fields generically written as  $\bar{\chi}_1 S \times \Gamma \chi_2$ , where  $S$  is a path of links and  $\Gamma$  is any Dirac matrix. We use interpolating fields of the so-called Gaussian smeared-form [27]

$$S = \left( \frac{1 + \kappa_G a^2 \Delta}{1 + 6\kappa_G} \right)^R,$$

where  $\kappa_G = 0.15$  is a hopping parameter,  $R = 30$  is the number of applications of the operator  $(1 + \kappa_G a^2 \Delta)/(1 + 6\kappa_G)$ , and  $\Delta$  the gauge-covariant 3-D Laplacian constructed from three-times APE-blocked links [28]. If necessary, we also incorporate in  $S$  a covariant derivative:

$$\nabla_i \equiv \frac{1}{2a} [U_i(x) - U_i^\dagger(x - \hat{i})].$$

It is the case to create a tensor meson.

The Dirac equations, which we then have to solve, read:

$$\left\{ \begin{array}{l} \sum_y D[f, r, \vec{\theta}]_{\alpha\beta}^{ab}(x, y) \phi[i, f, r, S, \vec{\theta}, \tilde{\alpha}, \tilde{t}]_{\beta}^b(y) = (S \eta[i])_{\alpha}^a(x) \delta_{\alpha\tilde{\alpha}} \delta_{t_x \tilde{t}} \\ \sum_y D[f_2, r_2, \vec{\theta}_2]_{\alpha\beta}^{ab}(x, y) \Phi[i, f_2, r_2, f_1, r_1, \Gamma_2, S_2, \vec{\theta}_2, \vec{\theta}_1, \tilde{\alpha}, \tilde{t}, \tilde{t} + t_S]_{\beta}^b(y) \\ \qquad \qquad \qquad = \Gamma_{2\alpha\beta} (S_2 \phi[i, f_1, r_1, \vec{\theta}_1, \tilde{\alpha}, \tilde{t}])_{\beta}^a(x) \delta_{t_S, t_x - \tilde{t}}. \end{array} \right.$$



We compute the “charged”  $B$  and  $D$  two-point correlators  $C_{\vec{\theta}; S_1 \Gamma_1; S_2 \Gamma_2}^{(2)hl}(t)$  which read [29]:

$$\begin{aligned} C_{\vec{\theta}; S_1 \Gamma_1; S_2 \Gamma_2}^{(2)hl}(t) &= \frac{1}{2} \sum_{r=\pm 1} \left\langle \text{Tr} \sum_{\vec{x}, \vec{y}} \Gamma_1 \mathcal{S}_l^{S_1}(r; \vec{y}, \vec{t}; \vec{x}, \vec{t}+t) \Gamma_2 \mathcal{S}_h^{S_2}(-r; \vec{x}, \vec{t}+t; \vec{y}, \vec{t}) \right\rangle, \\ &= \frac{1}{2} \sum_{r=\pm 1} \frac{1}{N} \sum_{n=1}^N \left\langle \text{Tr} \left\{ \sum_{\vec{x}} (\Gamma_1 \gamma_5)_{\tilde{\alpha}\tilde{\beta}} \phi^*[n, l, r, S_1, \vec{0}, \vec{\beta}, \vec{t}]_{\alpha}^b(\vec{x}, \vec{t}+t) \right. \right. \\ &\quad \left. \left. \times (\gamma_5 \Gamma_2)_{\alpha\beta} (S_2 \phi[n, h, r, \vec{\theta}, \vec{\alpha}, \vec{t}])_{\beta}^b(\vec{x}, \vec{t}+t) \right\} \right\rangle, \end{aligned}$$

where  $\langle \dots \rangle$  stands for the gauge ensemble average and  $h \equiv c$  or  $b$ .

We recall that, in Twisted-Mass QCD, quark propagators have the hermiticity property:

$$\mathcal{S}_q(r; x; y) = \gamma_5 \mathcal{S}_q^\dagger(-r; y; x) \gamma_5.$$

We also compute the “neutral”  $B \rightarrow D$  three-point correlators  $C_{\vec{\theta}; S_1 \Gamma_1; \Gamma; S_2 \Gamma_2}^{(3)b\Gamma c}(t, t_s)$  which read:

$$\begin{aligned} C_{\vec{\theta}; S_1 \Gamma_1; \Gamma; S_2 \Gamma_2}^{(3)b\Gamma c}(t, t_s) &= \frac{1}{2} \sum_{r=\pm 1} \left\langle \text{Tr} \sum_{\vec{x}, \vec{y}, \vec{z}} \Gamma \mathcal{S}_c(r, \vec{0}; \vec{z}, \vec{t}+t; \vec{y}, \vec{t}) \Gamma_1 \mathcal{S}_l^{S_1}(-r, \vec{0}; \vec{y}, \vec{t}; \vec{x}, \vec{t}+t_s) \right. \\ &\quad \left. \times \Gamma_2 \mathcal{S}_b^{S_2}(r, \vec{\theta}; \vec{x}, \vec{t}+t_s; \vec{z}, \vec{t}+t) \right\rangle, \\ &= \frac{1}{2} \sum_{r=\pm 1} \frac{1}{N} \sum_{n=1}^N \left\langle \text{Tr} \left\{ \sum_{\vec{x}} (\Gamma \gamma_5)_{\tilde{\alpha}\tilde{\beta}} (\phi[n, c, r, S_1, \vec{0}, \vec{\beta}, \vec{t}])_{\alpha}^b(\vec{x}, \vec{t}+t) \right. \right. \\ &\quad \left. \left. \times (\gamma_5 \Gamma_1)_{\alpha\beta} \Phi^*[n, b, -r, l, r, S_2, \Gamma_2, \vec{\theta}, \vec{0}, \vec{\alpha}, \vec{t}, \vec{t}+t_s]_{\beta}^b(\vec{x}, \vec{t}+t) \right\} \right\rangle. \end{aligned}$$

Those two types of correlators are depicted in Figure 1. On each of the two ensembles, we estimate the statistical error from a jackknife procedure.

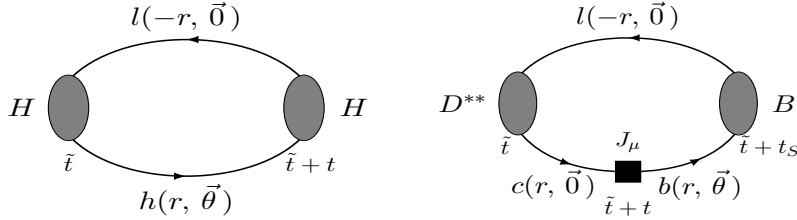


Figure 1: *Kinematical configuration of the 2-pt correlators (left) and 3-pt correlators (right) we compute.*

## 4 Masses and energies

We decide to concentrate our effort on the analysis of smeared-smeared two-pt correlators because the benefit of such a technique has been already clearly observed in a previous work by ETMC [30]. Masses and energies of pseudoscalar  $B$  and  $D$  mesons are first extracted from a fit of the form

$$C_{PP}(t, \vec{\theta}) = \frac{\mathcal{Z}^{2(1)}}{2E_P^{(1)}(\vec{\theta})} \left( e^{-E^{(1)}(\vec{\theta})t} + e^{-E^{(1)}(\vec{\theta})(T-t)} \right), \quad \mathcal{Z}^{2(1)} = \langle H^{(1)} | O_P^{H\dagger} | 0 \rangle,$$

in a time range where the contribution from the first excitation is small compared to the statistical error. The stability of the fit is checked by enlarging the time interval and adding a second exponential in the formula, i.e.:

$$C_{PP}(t, \vec{\theta}) = \sum_{i=1}^2 \frac{\mathcal{Z}^{2(i)}}{2E_P^{(i)}(\vec{\theta})} \left( e^{-E^{(i)}(\vec{\theta})t} + e^{-E^{(i)}(\vec{\theta})(T-t)} \right).$$

The last step in the analysis is to measure the effective energy  $E_P \equiv E_P^{(1)}$  of the ground state from the ratio

$$\frac{C_{PP}(t+1, \vec{\theta})}{C_{PP}(t, \vec{\theta})} = \cosh(E_P(\vec{\theta})) + \sinh(E_P(\vec{\theta})) \tanh[E_P(\vec{\theta})(t - T/2)].$$

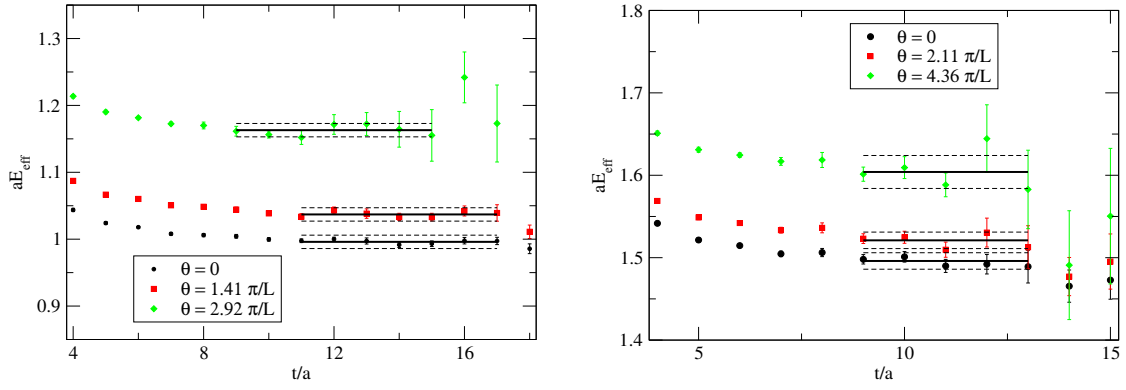


Figure 2: *Effective energies of "B"-mesons measured with the ETMC ensemble ( $\beta = 3.9$ ,  $\mu_{\text{sea}} = \mu_l = 0.0085$ ):  $\mu_h = 0.3498$  (left) and  $\mu_h = 0.6694$  (right).*

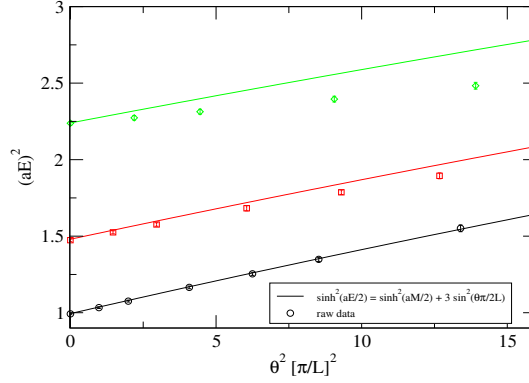


Figure 3: *Comparison of the "B"-mesons energies with the dispersion relation, at the ETMC ensemble ( $\beta = 3.9$ ,  $\mu_{\text{sea}} = \mu_l = 0.0085$ ). The energy have been rescaled to 1 for the lightest B at rest. The black, red and green points correspond to the three B masses in increasing order.*

We show in Figure 2 examples of plateaus for "B"-mesons energies at three different momenta. We study the dispersion relation to get an idea of the magnitude of cut-off effects. We show in Figure 3 the B meson energies and compare to the theoretical formula

$$\sinh^2[aE(\theta)/2] = \sinh^2[aM/2] + 3 \sin^2(\theta/2), \quad M \equiv E(0). \quad (4.1)$$

The agreement is good at the two lightest heavy masses but really bad at the heaviest one: cut-off effects are pretty large.

Interpolating fields of the  $2^+$  state are given by the formula  $O^{(\lambda)} = \epsilon_{\mu\nu}^{*(\lambda)} \bar{\chi}_c \gamma_\mu \nabla_\nu \chi_l$ ,  $\lambda = \pm 2, \pm 1, 0$ . Actually we choose to use linear combinations of those interpolating fields that read:

$$\left\{ \begin{array}{l} \tilde{O}^{(1)} = \frac{1}{\sqrt{2}}(O^{(+2)} + O^{(-2)}) = \frac{1}{\sqrt{2}} \bar{\chi}_c (\gamma_1 \nabla_1 - \gamma_2 \nabla_2) \chi_l \\ \tilde{O}^{(2)} = O^{(0)} = -\frac{1}{\sqrt{6}} \bar{\chi}_c (\gamma_1 \nabla_1 + \gamma_2 \nabla_2 - 2\gamma_3 \nabla_3) \chi_l \\ \tilde{O}^{(3)} = \frac{1}{\sqrt{2}}(O^{(+2)} - O^{(-2)}) = -\frac{i}{\sqrt{2}} \bar{\chi}_c (\gamma_1 \nabla_2 + \gamma_2 \nabla_1) \chi_l \\ \tilde{O}^{(4)} = \frac{1}{\sqrt{2}}(O^{(+1)} + O^{(-1)}) = \frac{i}{\sqrt{2}} \bar{\chi}_c (\gamma_2 \nabla_3 + \gamma_3 \nabla_2) \chi_l \\ \tilde{O}^{(5)} = \frac{1}{\sqrt{2}}(O^{(+1)} - O^{(-1)}) = -\frac{1}{\sqrt{2}} \bar{\chi}_c (\gamma_1 \nabla_3 + \gamma_3 \nabla_1) \chi_l \end{array} \right.$$

The two first interpolating fields live in the  $E$  representation of the  $O_h$  cubic group symmetry of rotations and inversion in a 3-d spatial lattice, while the three last live in the  $T_2$  representation of that group [31]. We finally consider the

$$C_{2^+,E}^{(2)}(t) = \frac{1}{2} \left[ \left\langle \sum_{\vec{x},\vec{y}} \tilde{O}_S^{(1)}(\vec{y}, t + \tilde{t}) \tilde{O}_S^{\dagger(1)}(\vec{x}, \tilde{t}) \right\rangle + \left\langle \sum_{\vec{x},\vec{y}} \tilde{O}_S^{(2)}(\vec{y}, t + \tilde{t}) \tilde{O}_S^{\dagger(2)}(\vec{x}, \tilde{t}) \right\rangle \right] \quad (4.2)$$

and

$$C_{2^+,T_2}^{(2)}(t) = \frac{1}{3} \left[ \left\langle \sum_{\vec{x},\vec{y}} \tilde{O}_S^{(3)}(\vec{y}, t + \tilde{t}) \tilde{O}_S^{\dagger(3)}(\vec{x}, \tilde{t}) \right\rangle + \left\langle \sum_{\vec{x},\vec{y}} \tilde{O}_S^{(4)}(\vec{y}, t + \tilde{t}) \tilde{O}_S^{\dagger(4)}(\vec{x}, \tilde{t}) \right\rangle + \left\langle \sum_{\vec{x},\vec{y}} \tilde{O}_S^{(5)}(\vec{y}, t + \tilde{t}) \tilde{O}_S^{\dagger(5)}(\vec{x}, \tilde{t}) \right\rangle \right]. \quad (4.3)$$

The masses we extract by studying the ratios  $\frac{C_{2^+,E}^{(2)}(t)}{C_{2^+,E}^{(2)}(t+1)}$  and  $\frac{C_{2^+,T_2}^{(2)}(t)}{C_{2^+,T_2}^{(2)}(t+1)}$  are in principal equal: any discrepancy comes from cut-off effects. We show in Figure 4 that, indeed, lattice artefacts are present.

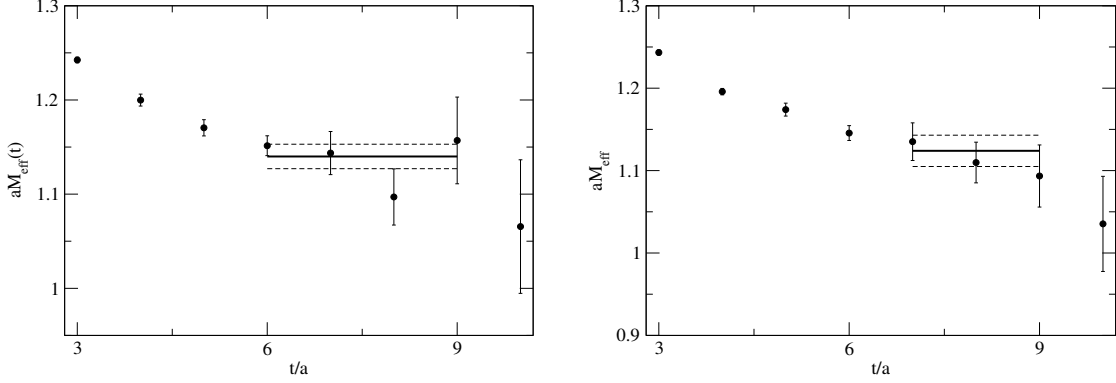


Figure 4: *Effective mass of the  $D_2^*$  meson measured with the ETMC ensemble ( $\beta = 3.9$ ,  $\mu_{\text{sea}} = \mu_l = 0.0085$ ):  $\frac{C_{2^+,E}^{(2)}(t)}{C_{2^+,E}^{(2)}(t+1)}$  (left) and  $\frac{C_{2^+,T_2}^{(2)}(t)}{C_{2^+,T_2}^{(2)}(t+1)}$  (right).*

As parity is broken by Twisted-mass action at finite lattice spacing [21] and the states we consider are not made with quarks of the same flavour doublet, contrary to what is discussed in section 5.2 of [22], the scalar  $D$  meson can in principle mix with the pseudoscalar  $D$  meson. We have to build a matrix of correlators  $\{C_{ij}(t)\}$  and solve a Generalised Eigenvalue Problem (GEVP) [32] - [34]. We study a  $2 \times 2$  system whose the entries correspond to the interpolating fields with Dirac structures  $\bar{\chi}_c \gamma^5 \chi_l$  and  $\bar{\chi}_c \chi_l$ :

$$C_{ij}(t) = \begin{bmatrix} C_{\bar{\chi}_c \gamma^5 \chi_l; \bar{\chi}_l \gamma^5 \chi_c}^{(2)}(t) & C_{\bar{\chi}_c \gamma^5 \chi_l; i \bar{\chi}_l \chi_c}^{(2)}(t) \\ C_{-i \bar{\chi}_c \chi_l; \bar{\chi}_l \gamma^5 \chi_c}^{(2)}(t) & C_{\bar{\chi}_c \chi_l; \bar{\chi}_l \chi_c}^{(2)}(t) \end{bmatrix}.$$

We solve the system

$$C_{ij}(t) v_j^{(n)}(t, t_0) = \lambda^{(n)}(t, t_0) C_{ij}(t_0) v_j^{(n)}(t, t_0). \quad (4.4)$$

We set  $t_0 = 3$  ( $\beta = 3.9$ ) and 5 ( $\beta = 4.05$ ).  $\lambda^{(n)}(t, t_0)$  and  $v^{(n)}(t, t_0)$  are the eigenvalues and eigenvectors of the matrix  $C^{-1}(t_0)C(t)$ . The effective mass  $m_{D_0^*}$  of the scalar meson is given by:

$$\lambda^{(2)}(t, t_0) = \frac{\cosh[m_{D_0^*}(T/2 - t)]}{\cosh[m_{D_0^*}(T/2 - t_0)]}. \quad (4.5)$$

We show in Figure 5  $m_{D_0^*}$  for the ensemble ( $\beta = 3.9$ ,  $\mu_{\text{sea}} = 0.0085$ ). The signal is unfortunately quite short, but still acceptable for our qualitative study.

We collect in the Appendix all the masses and energies that we extract in our analysis. The total error includes the statistical one and the discrepancy of results when we change the time range  $[t_{\min}, t_{\max}]$  of fits by  $t_{\min} \pm 1$  and  $t_{\max} \pm 1$ , when we take different  $t_0$  in the range  $[3, 6]$  and, in the case of pseudoscalar  $B$  mesons, when we perform a 2-states exponential fit.

#### 4.1 $M_{D_2^*} - M_D$ and $M_{D_0^*} - M_D$ in the continuum limit and experiment

In Table 6 in the appendix we give the masses of the  $D_2^*$ ,  $D_0^*$  and  $D$  mesons. It is interesting to perform an extrapolation to the continuum and compare with the experimental data. For the latter we will take the  $c\bar{s}$  mesons. It does not change

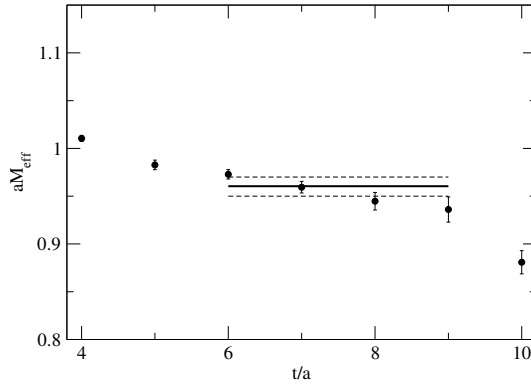


Figure 5: *Effective mass of the  $D_0^*$  meson measured with the ETMC ensemble ( $\beta = 3.9$ ,  $\mu_{\text{sea}} = \mu_l = 0.0085$ ).*

anything for the tensor meson as compared to the non-strange charmed mesons ( $M_{D_2^*}(2460) - M_D \simeq M_{D_{2s}^*}(2573) - M_{D_s}$ ) but for the scalar mesons we gain since the  $D_{0s}^*(2317)$  has a narrow and clear signal which is not the case of the  $D_0^*(2400)$  which has a very broad signal due to its S-wave decay into  $D\pi$ .

lattice spacing (fm)	inverse spacing (GeV)	scalar	tensor
0.085(3)	2.32(8)	0.55(4)(2)	0.81(6)(3)
0.069(2)	2.86(8)	0.42(1)(1)	0.87(3)(3)
0.0	inf	0.18(8)(12)	0.98(14) $\left(\begin{smallmatrix} +6 \\ -12 \end{smallmatrix}\right)$
Exp.		0.349	0.605

Table 3: *Mass differences  $M_{D_0^*} - M_D$  (third column) and  $M_{D_2^*} - M_D$  (fourth column) for  $\beta = 3.9$  (first line) and  $\beta = 4.05$  (second line). We use the lattice spacings reported in Table 2. The extrapolation to vanishing lattice spacing is in the third line and the experimental data  $M_{D_{0s}^*}(2317) - M_{D_s}$  and  $M_{D_{2s}^*}(2573) - M_{D_s}$  are in the fourth line. The lattice spacings are taken from Table 2. The first error corresponds to the statistical error, the second to the uncertainty on the lattice spacing. As we see the dependence of the value extrapolated to continuum strongly depends on one sigma variations in the lattice spacing. Unluckily the lattice spacing ratio between  $\beta = 3.9$  and  $\beta = 4.05$  which optimises the agreement with experiment for  $M_{D_0^*} - M_D$  is the opposite to the one which optimises  $M_{D_2^*} - M_D$ .*

We perform the extrapolation to the continuum limit and compute the error using jackknife. We show our results in Table 3. We see that the agreement with experiment is not good but also strongly dependent on small variations in the lattice spacings. For the moment we cannot say much, except that more statistics and smaller lattice spacings would help in settling this issue. A similar conclusion was made recently in a lattice study with  $N_f = 2 + 1 + 1$  dynamical quarks regularised by TmQCD [37].

## 5 $B$ decay to the scalar $D_0^*$ charmed meson

In this section we will restrict to the zero recoil kinematics, in other words the initial  $B$  meson is taken at rest. We restrict ourselves to this simpler case because the momentum dependance of the  $B \rightarrow D_0^*$  decay is very difficult to study on the lattice (3-pt correlators are very noisy) and we cannot yet say anything significant about it, but also because the non vanishing of the zero recoil amplitude is of utmost phenomenological significance : in the infinite momentum limit, the  $B \rightarrow D_0^*$  amplitude vanishes at zero recoil [13]. This forbids the decay into a S-wave between the lepton pair and the  $D_0^*$  and S-wave since an S-wave clearly does not vanish at zero recoil. The S-wave is a significant contribution for these decays since their available phase space is rather small, and higher waves are suppressed by the so-called centrifugal barrier effect. With finite heavy quark masses we will show that the zero recoil amplitude *does not vanish*, there is a non vanishing S-wave and this may change drastically the ratio between  $\Gamma(B \rightarrow D_2^*)$  and  $\Gamma(B \rightarrow D_0^*)$  since the  $B \rightarrow D_2^*$  decay amplitude does vanish at zero recoil whether the mass of the  $c$  and  $b$  is taken infinite or finite, thus implying only a D-wave decay. The possible importance of a non vanishing zero recoil amplitude was stressed in [35] where the authors estimated subleading corrections to the infinite mass limit : although subleading in the  $\Lambda/m_{c,b}$  expansion, the S-wave may not be negligible.

## 5.1 Computation of the $\Gamma(B \rightarrow D_0^*)$ over $\Gamma(B \rightarrow D)$ ratio at zero recoil

We will compute the ratio  $\Gamma(B \rightarrow D_0^*)/\Gamma(B \rightarrow D)$ . We take  $\Gamma(B \rightarrow D)$  as a benchmark since it is experimentally fairly well known, and  $D$  being a  $J = 0$  state as  $D_0^*$ , it is expected that the momentum dependence of these decays will be rather similar. We recall some formulae neglecting for the moment the  $D - D_0^*$  mixing due to the parity violation at finite lattice spacing when using twisted mass quarks. The matrix elements  $\langle B|V_0|D \rangle$  and  $\langle B|A_0|D_0^* \rangle$  are given by the following ratio

$$\langle B|O|H_c \rangle = \frac{C_{\text{BOH}_c}^{(3)}(t_p, t, t_s) \sqrt{Z_{H_c}/Z_B} Z_O}{C_{H_c}^{(2)}(t - t_s) \exp(-E_B(t_p - t)) / (2E_B)}, \quad (5.1)$$

where  $t_s < t < t_p$  are respectively the source, current and sink times (cf Fig 1).

$Z_0 = Z_V(Z_A)$  when  $H_c = D(D_0^*)$ .  $Z_{H_c}$  and  $Z_B$  are defined from the fit of the 2-pt correlators of the  $H_c$  and  $B$  mesons, assuming we are far enough from the center of the lattice to be allowed to neglect the backward exponential in time while the contribution of excited states is small.

$$C_B^{(2)}(t, \vec{\theta}) = \frac{Z_B}{2E_B(\vec{\theta})} \exp(-E_B(\vec{\theta})t); \quad C_{H_c}^{(2)}(t, 0) = \frac{Z_{H_c}}{2M_{H_c}} \exp(-M_{H_c}t). \quad (5.2)$$

Then we compute

$$\frac{\langle B|A_0|D_0^* \rangle}{\langle B|V_0|D \rangle} = \frac{C_{\text{BA}_0D_0^*}^{(3)}(t_p, t, t_s) C_D^{(2)}(t - t_s) Z_A \sqrt{Z_{D_0^*}}}{C_{\text{BV}_0D}^{(3)}(t_p, t, t_s) C_{D_0^*}^{(2)}(t - t_s) Z_V \sqrt{Z_D}}. \quad (5.3)$$

$v^{(1)}$	$v^{(2)}$
0.97	-0.3 i
-0.24 i	0.95

Table 4: Values of the approximately orthonormalised eigenvectors  $v^{(1)}$  and  $v^{(2)}$ , eq. (4.5), for  $\beta = 3.9$ ,  $t_0 = t_s = 3$ ,  $t = 7$  and  $t_p = 14$ .  $v^{(1)}v^{(2)\dagger} = 0.07i$ , rather small as expected in eq 5.4.

## 5.2 Taking into account the scalar-pseudoscalar mixing

In section 4 we have detailed the Generalised Eigenvalue method. As explained there and in section 3, we restrict ourselves to a  $2 \times 2$  matrix of smeared and stochastic 2-pt correlators. The largest (smallest) eigenvalue  $\lambda^{(1)}$  ( $\lambda^{(2)}$ ) will be related to the mass of the  $D$  ( $D_0^*$ ) state. The corresponding eigenvectors give the linear combination of  $\bar{\chi}_c \gamma_5 \chi_l$  and  $\bar{\chi}_c \chi_l$  interpolating fields that have the largest coupling to the  $D(D_0^*)$  state. The eigenvectors turn out to be not far from orthogonal

$$v^{(1)}v^{(2)\dagger} = \sum_{k=1,2} v_k^{(1)} v_k^{(2)*} = 0.07i \simeq 0, \quad (5.4)$$

as seen for example in table 4. One might say that 0.07 is not so small but this is not surprising, since there are other states in which the B might decay than only the ground state scalar and pseudoscalar that we consider in our analysis. We can thus to a fair approximation orthonormalise the eigenvectors so that

$$v^{(i)}v^{(j)\dagger} \simeq \delta_{i,j}, \quad (5.5)$$

without changing the eigenvalues, since in eq (4.4) the same factor multiplies both sides of the equation. Thus, we define the 2-pt correlator of  $D_0^*$  meson by

$$\begin{aligned} \lambda^{(2)}(t - t_s, t_0) \sum_{i,j=1}^2 v_i^{(2)\dagger}(t - t_s, t_0) C_{ij}^{(2)}(t_0) v_j^{(2)}(t - t_s, t_0) &= \sum_{i,j=1}^2 v_i^{(2)\dagger}(t - t_s, t_0) C_{ij}^{(2)}(t - t_s) v_j^{(2)}(t - t_s, t_0), \\ \lambda^{(1)}(t - t_s, t_0) \sum_{i,j=1}^2 v_i^{(1)\dagger}(t - t_s, t_0) C_{ij}^{(2)}(t_0) v_j^{(1)}(t - t_s, t_0) &= \sum_{i,j=1}^2 v_i^{(1)\dagger}(t - t_s, t_0) C_{ij}^{(2)}(t - t_s) v_j^{(1)}(t - t_s, t_0), \end{aligned} \quad (5.6)$$

where we fit with

$$\lambda^{(2)}(t-t_s, t_0) = \frac{Z_{D_0^*}}{2M_{D_0^*}} \exp(-M_{D_0^*}(t-t_s-t_0)) \quad \lambda^{(1)}(t-t_s, t_0) = \frac{Z_D}{2M_D} \exp(-M_D(t-t_s-t_0)). \quad (5.7)$$

Defining

$$\begin{aligned} v_i^{(2)\dagger}(t-t_s, t_0) C_{ij}^{(2)}(t-t_s) v_j^{(2)}(t-t_s, t_0) &= \frac{Z_2^{(2)}}{2M_{D_0^*}} \exp(-M_{D_0^*}(t-t_s)), \\ v_i^{(1)\dagger}(t-t_s, t_0) C_{ij}^{(2)}(t-t_s) v_j^{(1)}(t-t_s, t_0) &= \frac{Z_1^{(1)}}{2M_{D_0^*}} \exp(-M_D(t-t_s)), \end{aligned} \quad (5.8)$$

we get from eq. (5.6, 5.7)

$$\begin{aligned} Z_2^{(2)} &= \exp(M_{D_0^*} t_0) Z_{D_0^*} v_i^{(2)\dagger}(t-t_s, t_0) C_{ij}^{(2)}(t_0) v_j^{(2)}(t-t_s, t_0), \\ Z_1^{(1)} &= \exp(M_D t_0) Z_D v_i^{(1)\dagger}(t-t_s, t_0) C_{ij}^{(2)}(t_0) v_j^{(1)}(t-t_s, t_0). \end{aligned} \quad (5.9)$$

### 5.2.1 Symmetry properties of the matrix elements

In the continuum it is obvious by parity conservation that

$$\langle B|A_0|D \rangle = \langle B|V_0|D_0^* \rangle = 0 \quad (5.10)$$

However parity is not conserved by the twisted mass quark action at finite lattice spacing. But this action has an exact symmetry [21], the flavour-parity

$$\mathcal{P}_5^{\text{SP}} \equiv \mathcal{P} \otimes (\mu_l, \mu_c, \mu_b \rightsquigarrow -\mu_l, -\mu_c, -\mu_b) \quad (5.11)$$

where  $\mathcal{P}$  is the spatial parity, and  $\mu_l, \mu_c, \mu_b$  are the twisted mass terms for the light, charm and beauty quarks. We assume we are at maximal twist (vanishing of  $m_{\text{PCAC}}$ ). Therefore if we use

$$C_{i,j,k}^{(3)\text{sym}}(t_p, t, t_s) \equiv (1 + \mathcal{P}_5^{\text{SP}}) C_{i,j,k}^{(3)}(t_p, t, t_s) \quad (5.12)$$

we get the validity of eq. (5.10) also for finite lattice spacing. This symmetrisation will be assumed in the following.

### 5.2.2 GEVP on the 3 pt correlators

In this section we assume  $t_s < t < t_p$  and  $t_0 \leq t - t_s$ . Starting from the 3-pt correlators  $C_{BA_0(V_0)O_i}^{(3)}(t_p, t, t_s) = \langle \bar{\chi}_b \gamma_5 \chi_l(t_p) A_0(V_0)(t) O_i(\bar{\chi}_c, \chi_l, t_s) \rangle$ ,  $O_i(\bar{\chi}_c, \chi_l) \equiv \{\bar{\chi}_c \gamma_5 \chi_l, \bar{\chi}_c \chi_l\}$  and following the authors [36] in their way of extracting the decay constant  $f_B$ , we consider the projected 3-pt correlators

$$\begin{aligned} C_{BA_0 D_0^*}^{(3)'}(t_p, t, t_s) &= \frac{\langle \bar{\chi}_b \gamma_5 \chi_l(t_p) A_0(t) \bar{\chi}_c \chi_l(t_s) v_{\bar{\chi}_c \chi_l}^{(2)}(t-t_s, t_0) \rangle}{\sqrt{v_i^{\dagger(2)}(t-t_s, t_0) C_{ij}^{(2)}(t-t_s) v_j^{(2)}(t-t_s, t_0)}} \\ &\times \left( \frac{\lambda^{(2)}(t_0 + a, t_0)}{\lambda^{(2)}(t_0 + 2a, t_0)} \right)^{(t-t_s)/2a} \frac{2E_B e^{(t_p-t)E_B}}{\sqrt{Z_B}} \sqrt{2m_{D_0^*}}, \\ C_{BV_0 D}^{(3)'}(t_p, t, t_s) &= \frac{\langle \bar{\chi}_b \gamma_5 \chi_l(t_p) V_0(t) \bar{\chi}_c \gamma_5 \chi_l(t_s) v_{\bar{\chi}_c \gamma_5 \chi_l}^{(1)}(t-t_s, t_0) \rangle}{\sqrt{v_i^{\dagger(1)}(t-t_s, t_0) C_{ij}^{(2)}(t-t_s) v_j^{(1)}(t-t_s, t_0)}} \\ &\times \left( \frac{\lambda^{(1)}(t_0 + a, t_0)}{\lambda^{(1)}(t_0 + 2a, t_0)} \right)^{(t-t_s)/2a} \frac{2E_B e^{(t_p-t)E_B}}{\sqrt{Z_B}} \sqrt{2m_D}. \end{aligned} \quad (5.13)$$

We remind that the normalisation factor  $Z_2^{(2)}$  cancels between  $\langle \bar{\chi}_b \gamma_5 \chi_l(t_p) A_0(V_0)(t) \bar{\chi}_c (\gamma_5) \chi_l(t_s) \rangle$  and  $\sqrt{v_i^{\dagger(2(1))}(t-t_s, t_0) C_{ij}^{(2)}(t-t_s) v_j^{(2(1))}(t-t_s, t_0)}$  while the factor  $\left( \frac{\lambda^{(2(1))}(t_0+a, t_0)}{\lambda^{(2(1))}(t_0+2a, t_0)} \right)^{(t-t_s)/2a} \sim e^{-E_{D_0^*(D)}(t-t_s)/2a}$  compensates the residual time exponential dependence. We do not take into account the contributions  $\propto v_{\bar{\chi}_c \gamma_5 \chi_l}^{(2)}(t-t_s, t_0)$  and  $v_{\bar{\chi}_c \chi_l}^{(1)}(t-t_s, t_0)$  to the projected correlators  $\sum_i \langle \bar{\chi}_b \gamma_5 \chi_l(t_p) A_0(V_0)(t) O_i(\bar{\chi}_c, \chi_l, t_s) v_i^{(2(1))}(t-t_s, t_0) \rangle$  because the B meson goes through operator  $A_0$  ( $V_0$ ) only to a pure scalar (pseudoscalar) state.

The ratio in eq. 5.3 becomes

$$\frac{\langle B|A_0|D_0^* \rangle}{\langle B|V_0|D \rangle} \simeq \frac{C_{BA_0 D_0^*}^{(3)'}(t_p, t, t_s)}{C_{BV_0 D}^{(3)'}(t_p, t, t_s)} \times \frac{Z_A}{Z_V} \frac{\sqrt{2m_{D_0^*}}}{\sqrt{2m_D}}, \quad (5.14)$$

using eq (5.7)

Of course the ratio of branching fractions has to take into account the difference in phase space. However, we ignore totally the dependence of the amplitude on the recoil, having only estimated the zero recoil contribution. Therefore, we will for the moment neglect the phase space dependence. We collect the results of eq. 5.14 in Table 5 and show plateaus in Figure 6.

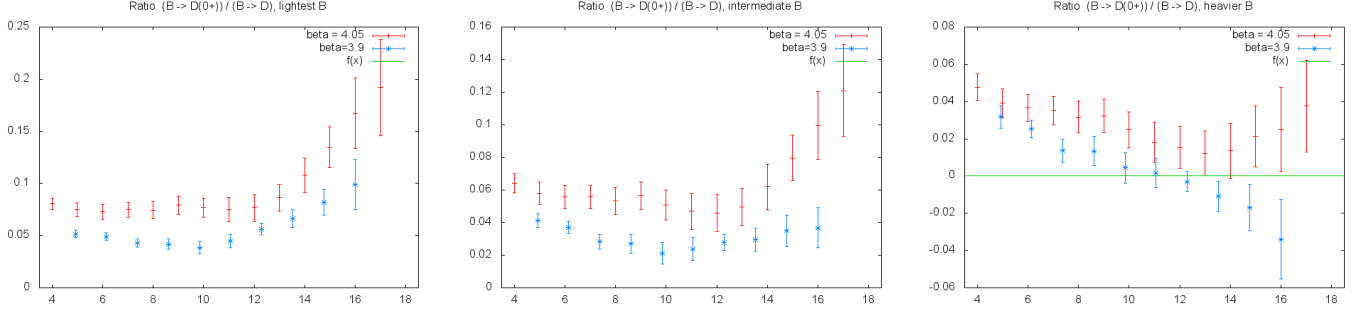


Figure 6: The ratio in eq. (5.14) once symmetrised according to Eq. (5.12) for the three  $b$  quark masses and for both lattice spacings. The times at  $\beta = 4.05$  have been rescaled to have equal physical times for both  $\beta$ 's at a given position on the time axis. To check the independence on the time  $t_0$  we show the computation with  $t_0 = 3, 4$  ( $t_0 = 4, 5$ ) for  $\beta = 3.9$  ( $\beta = 4.05$ ). We see acceptable plateaus rather similar for both  $\beta$ 's at small times, say  $t < 9$  ( $t < 11$ ) in units of  $\beta = 3.9$  ( $\beta = 4.05$ ) lattice spacings. For larger times the agreement is lost.

The values of the plateaus are reported in table 5. The dependence in  $m_B$  agrees with the formula  $c/m_B + b$ . We show both the extrapolation to the physical  $B$  meson and also to the vanishing lattice spacing. When both extrapolations are combined we get a ratio of 0.15(20). In this limit we have more than 100% error. This is due to the fact that the ratios decrease with the  $B$  meson mass, the error staying rather stable leading to a large noise/signal ratio. It is also seen that the noise/signal ratio increases significantly when extrapolating to zero lattice spacing, because we only use two lattice spacings which are too far from 0.

As a gross estimate the ratio of branching fractions is the square of the ratio of amplitudes reported in Table 5. The experimental value of the ratios of branching fractions can be very grossly estimated to be around 0.1-0.2 which would correspond to a ratio of amplitudes  $\sim 0.3 - 0.45$ . This does not contradict our estimate. At this point we must remain very careful : the experimental status of the  $D_0^*$  is unclear, the resonance being very broad, and our theoretical estimate is affected by very large uncertainties. Better statistics and one additional smaller lattice spacing will improve the latter point.

$\beta$	ratio $m_{b(1)}$	ratio $m_{b(2)}$	ratio $m_{b(3)}$	ratio at physical B
3.9	0.33(5)	0.24(4)	0.16(4)	0.06(4)
4.05	0.40(4)	0.31(4)	0.20(4)	0.09(4)
continuum	0.55(16)	0.45(17)	0.29(18)	0.15(20)

Table 5: We give the ratios defined in eq. (5.14) averaged over what seems a good plateau : 6-9 (5-11) for  $\beta = 3.9$  ( $\beta = 4.05$ ). The  $b$  quarks range from the lightest to heaviest from left to right :  $m_B \simeq 2.5, 3, 3.7$  GeV. The right column corresponds to the extrapolation at the physical  $B$  mass, 5.2 GeV. The last line corresponds to the extrapolation to the continuum.

## 6 $B$ decay to the tensor ( $J = 2^+$ ) charmed meson

In this section we want to estimate the amplitudes for  $B \rightarrow D_2^* \ell \nu$  ( $B_s \rightarrow D_{s2}^* \ell \nu$ ) decays. In [1] the spin-two charmed mesons are named  $D_2^*(2460)$  ( $D_{s2}^*(2573)$ ). For the initial  $B$  meson, we use three " $B_i$ ,  $i = 1, 2, 3$ " with increasing masses in the range 2.5, 3.0 and 3.7 GeV. As was mentioned before, the " $B_i$ ,  $i = 1, 2, 3$ " are moving while the final charmed meson is at rest. We concentrate on the calculation of the form factor  $\tilde{k}$  since it was shown in section 2.5 that it is, by large, dominant in the decay width.

## 6.1 3-pt correlators computed for $B \rightarrow D(2^+)$

We start from the formulae recalled in section 2.5. We use a symbolic notation to represent the hadronic matrix elements

$$H_{i,j,k} = \langle B | A_k | D_2^* (\epsilon_{ij}^{(\lambda)}) \rangle \quad \rightsquigarrow \quad A_k V_j D_i.$$

The various combinations to extract  $\tilde{k}$  are collected in Table 6. We consider all of these combinations and average the resulting value for  $\tilde{k}$ . To eliminate artefacts we must also apply the symmetrized result according to Eq. (5.12)

combination	expression
$p\tilde{k} = -\sqrt{6}\mathcal{T}_{1(0)}^A$	$A_1 V_1 D_1 + A_1 V_2 D_2 - 2 A_1 V_3 D_3$
$p\tilde{k} = -\sqrt{6}\mathcal{T}_{2(0)}^A$	$A_2 V_1 D_1 + A_2 V_2 D_2 - 2 A_2 V_3 D_3$
$p\tilde{k} = \sqrt{6}/2 \mathcal{T}_{3(0)}^A$	$-(A_3 V_1 D_1 + A_3 V_2 D_2 - 2 A_3 V_3 D_3)/2$
$p\tilde{k} = [\mathcal{T}_{1(+2)}^A + \mathcal{T}_{1(-2)}^A]$	$(A_1 V_1 D_1 - A_1 V_2 D_2)/2$
$p\tilde{k} = -[\mathcal{T}_{2(+2)}^A + \mathcal{T}_{2(-2)}^A]$	$-(A_2 V_1 D_1 - A_2 V_2 D_2)/2$
$p\tilde{k} = i \left\{ [\mathcal{T}_{1(+2)}^A - \mathcal{T}_{1(-2)}^A] + [\mathcal{T}_{1(+1)}^A + \mathcal{T}_{1(-1)}^A] \right\}$	$A_1 V_1 D_2 + A_1 V_2 D_1 - A_1 V_3 D_2 - A_1 V_2 D_3$
$p\tilde{k} = -i \left\{ [\mathcal{T}_{3(+2)}^A - \mathcal{T}_{3(-2)}^A] + [\mathcal{T}_{3(+1)}^A + \mathcal{T}_{3(-1)}^A] \right\}$	$-A_3 V_1 D_2 - A_3 V_2 D_1 + A_3 V_3 D_2 + A_3 V_2 D_3$
$p\tilde{k} = i \left\{ [\mathcal{T}_{1(+1)}^A + \mathcal{T}_{1(-1)}^A] + i [\mathcal{T}_{1(+1)}^A - \mathcal{T}_{1(-1)}^A] \right\}$	$A_1 V_1 D_3 + A_1 V_3 D_1 - A_1 V_3 D_2 - A_1 V_2 D_3$
$p\tilde{k} = -i \left\{ [\mathcal{T}_{2(+1)}^A + \mathcal{T}_{2(-1)}^A] + i [\mathcal{T}_{2(+1)}^A - \mathcal{T}_{2(-1)}^A] \right\}$	$-A_2 V_1 D_3 - A_2 V_3 D_1 + A_2 V_3 D_2 + A_2 V_2 D_3$
$p\tilde{k} = i \left\{ [\mathcal{T}_{2(+2)}^A - \mathcal{T}_{2(-2)}^A] + i [\mathcal{T}_{2(+1)}^A - \mathcal{T}_{2(-1)}^A] \right\}$	$A_2 V_1 D_2 + A_2 V_2 D_1 - A_2 V_3 D_1 - A_2 V_1 D_3$
$p\tilde{k} = -i \left\{ [\mathcal{T}_{3(+2)}^A - \mathcal{T}_{3(-2)}^A] - i [\mathcal{T}_{3(+1)}^A - \mathcal{T}_{3(-1)}^A] \right\}$	$-A_3 V_1 D_2 - A_3 V_2 D_1 + A_3 V_3 D_1 + A_3 V_1 D_3$

Table 6: *Combinations of 3-pt correlators used to extract  $\tilde{k}$ .*

## 6.2 Subtracting zero momentum 3 point correlators

The 3-pt correlation functions involving a tensor  $D$  meson are unfortunately very noisy : hence it is extremely difficult to get a large enough signal-to-noise ratio. We will use a trick <sup>5</sup> which consists in subtracting to every 3-pt correlator the correlator with the same gauge configuration and the same operators at zero momentum. Indeed we know that the decay  $B \rightarrow D_2^*$  vanishes at zero recoil. This is obvious in the continuum limit since we start with a  $B$  meson of vanishing angular momentum  $J$ . The weak interaction operator (axial current  $A_\mu$ ) having  $J = 0$  for  $A_0$  and  $J = 1$  for  $A_i$  ( $i = 1, 2, 3$ ), cannot generate a  $J = 2$  state : at zero recoil there is no momentum to generate a higher angular momentum.

However this vanishing is also exact on a lattice. The proof goes as follows: the 3-pt correlators which contribute to the  $D_2^* \rightarrow B$  are linear combinations of correlators of the type

$$C_{i,j,k}^{(3)}(t_p, t, t_s) = \langle O_B(t_p) A_k(t) O_{D_i V_j}(t_s) \rangle. \quad (6.1)$$

where  $i, j, k \in \{1, 2, 3\}$  may be different or equal. All operators are at rest (zero recoil). We have assumed the  $D_2^*$  meson ( $B$  meson) interpolating field to be at the source time  $t_s$  (sink time  $t_p$ ), and the current at time  $t$  with  $t_p \geq t \geq t_s$ .

Let us choose one of the three spatial directions  $\hat{l}$  and consider the rotation  $\mathcal{R}_l(\pi)$  of angle  $\pi$  around it : the spatial coordinates perpendicular to  $\hat{l}$  change sign. All vector operators,  $D_i, V_i$ , and  $A_i$  change sign if  $i$  is perpendicular to  $\hat{l}$  whereas they remain unchanged if  $i = l$ .

$\mathcal{R}_l(\pi)$  belongs to the 3-D cubic symmetry group. The lattice actions are invariant under  $\mathcal{R}_l(\pi)$ , even the twisted mass action since  $\mathcal{R}_l(\pi)$  is parity even. In equation (6.1), there are three operators at three different times. Being at rest, we may assume that their spatial nesting is invariant under  $\mathcal{R}_l(\pi)$  : it can be a stochastic source, a local operator at the origin of 3-space, a smeared operator symmetric around the origin of 3-space or a local operator integrated over 3-space

<sup>5</sup>We are indebted to Philippe Boucaud who suggested this trick.



(for the current). If an odd number among the indices  $i, j, k$  are perpendicular to  $\hat{l}$ , then the correlator in Eq. (6.1) changes sign under  $\mathcal{R}_l(\pi)$  and the amplitude must vanish. This happens if  $i = j = k$ ,  $\hat{l}$  being any other direction or if  $i = j \neq k$ ,  $l = i$ .

However, if  $i, j, k$  are all different it does not work : any  $\mathcal{R}_l(\pi)$  will keep the  $C^{(3)}$  of Eq. (6.1) unchanged and thus cannot be proven to vanish on the lattice although it should in the continuum limit. This type of term does generate lattice artefacts. A parity operation would change its sign (changing the sign of all three operators) but parity is not an invariant of the twisted mass action. We must then use correlators symmetrised according to the exact symmetry of twisted mass action [21] i.e. apply Eq. (5.12) : the lattice artefact should then disappear and  $C_{i,j,k}^{(3)\text{sym}}(t_s, t_c, t_p) = 0$  on the lattice, at zero recoil.

Since it must vanish at zero recoil on the lattice, we may subtract to the three point correlator at non vanishing recoil the same configuration at zero recoil. This reduces some correlated noise, and indeed it turns out that the signal, although still very noisy, is significantly improved. We have computed the three point functions with both all  $\mu$ 's positive (set  $sp_0$ ) and all opposite in sign (set  $sp_1$ ). It turns out that the real parts of the 3-point functions are very similar for both  $sp_0$  and  $sp_1$  sets, while the imaginary parts are approximatively opposite in signs, from which we can guess that the contributions with  $i, j, k$  not all different are dominantly real while the ones with  $i, j, k$  different are dominantly imaginary. This is related to the fact that the terms odd in the  $\mu$ 's have an  $i$  with respect to the ones which are even, but for the sake of brevity we will skip an exact proof.

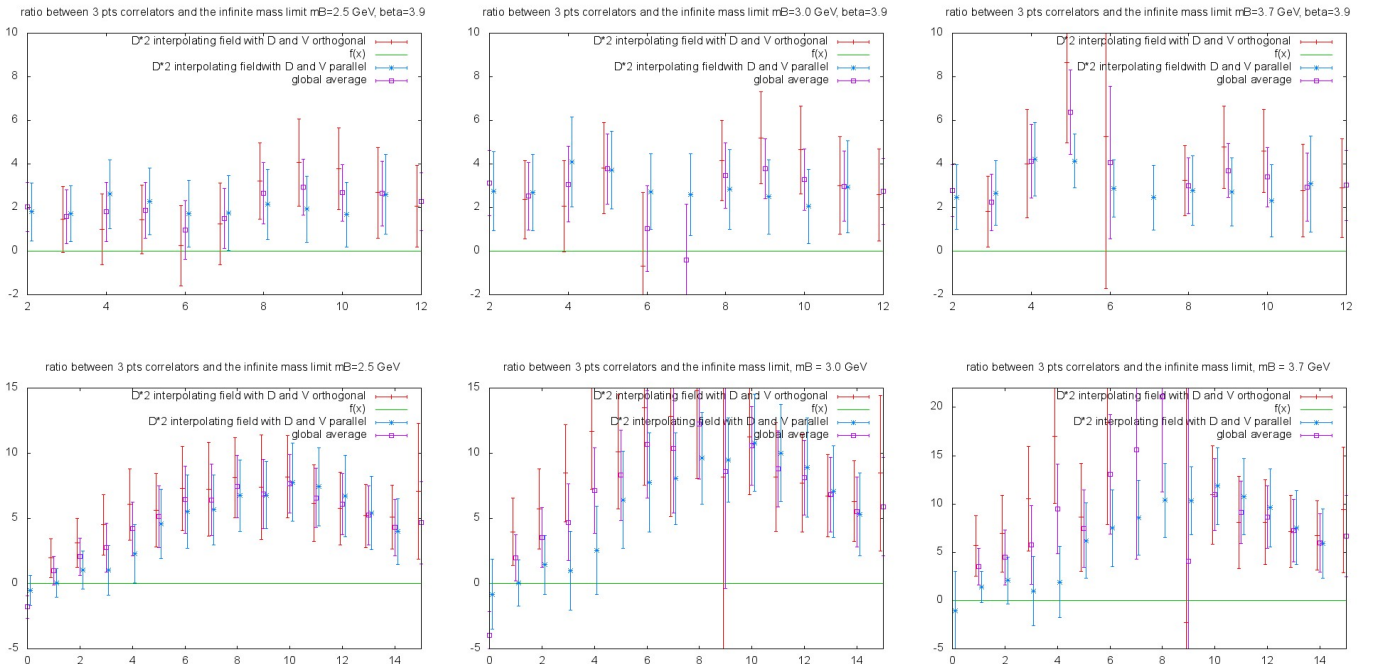


Figure 7: The ratio of the three point function for  $B \rightarrow D_2^*$  over the value derived from the infinite mass limit, Eq. (6.6), once the three point function has been symmetrised according to Eq. (5.12) and once the three point function at zero recoil has been subtracted. We show the three  $b$  quark masses. The upper three plots correspond to  $\beta = 3.9$  and  $t_p - t_s = 14$ . The lower plots to  $\beta = 4.05$  and  $t_p - t_s = 18$ . We use for the three point functions the combinations expanded in table 6, the average of the five first lines is represented by the blue star, it corresponds to the discrete representation  $E^+$  for the  $D_2^*$  interpolating field,  $D_i V_i$ , while in red are the average of the six last lines of table 6, discrete representation  $T_2^+$  i.e.  $D_i V_j, j \neq i$ . The full average is the purple square.

### 6.3 Extracting the matrix element

An estimate of  $p \tilde{k}$  is thus given by:

$$R_{i,D_2^*,\vec{\theta}}(t_p, t, t_s) = \frac{C_{B(\vec{\theta})A_i D_2^*}^{(3)}(t_p, t, t_s) \sqrt{Z_B Z_{D_2^*}} Z_A}{C_{D_2^*}^{(2)}(t - t_s) C_{B(\vec{\theta})}^{(2)}(t_p - t)}, \quad (6.2)$$

where the 3-pt correlators are the combinations of correlators listed in table 6, symmetrised according to Eq. (5.12) and with the corresponding zero recoil 3-pt correlators subtracted. Let us remind that  $\vec{p} = \vec{\theta} \pi / L$  where  $L$  is the spatial length

of the lattice. We have used systematically  $\vec{\theta}_x = \vec{\theta}_y = \vec{\theta}_z = \theta$  whence  $|\vec{p}| = \sqrt{3}\theta\pi/L$ . In fact we prefer to present another ratio. Since the estimate of  $B \rightarrow D_2^*$  in the infinite mass limit is rather successful, in good agreement with experiment, we will compute the ratio of the 3-pt correlators divided by the one which is derived from the infinite mass limit formula [7]:

$$\tau_{3/2}(w) = \tau_{3/2}(1) \left( \frac{2}{1+w} \right)^{2\sigma_{3/2}^2}. \quad (6.3)$$

Where the fit gives  $\sigma_{3/2}^2 \simeq 1.5$ , and  $\tau_{3/2}(1) \simeq 0.539$  and the formula in section 2.5.1

$$\tilde{k}_{\text{inf}} = \sqrt{3} \sqrt{r_{D_2^*}} (1+w) \tau_{3/2}(w), \quad (6.4)$$

with  $r_{D_2^*} = M_{D_2^*}/M_B$ . This  $\tilde{k}_{\text{inf}}$  will be used as a benchmark for  $\tilde{k}$  extracted from our present calculations. From our benchmark  $\tilde{k}_{\text{inf}}$  we compute the benchmark three point correlator, the  $D_2^*$  meson being created at time  $t_s$  the current inserted at time  $t$  and the  $B$  annihilated at time  $t_p$ :

$$C_{\text{inf}}^{(3)}(t_p, t, t_s) = \tilde{k}_{\text{inf}} |\vec{p}| C_{D_2^*}^{(2)}(t - t_s) C_B^{(2)}(t_p - t) Z_A / \sqrt{Z_B Z_{D_2^*}}. \quad (6.5)$$

We thus consider the ratio

$$\frac{\tilde{k}}{\tilde{k}_{\text{inf}}} = \frac{C_{B(\vec{\theta})A_i D_2^*}^{(3)}(t_p, t, t_s)}{C_{\text{inf}}^{(3)}(t_p, t, t_s)}. \quad (6.6)$$

To increase the signal we take the average on the 11 expressions for  $\tilde{k}$  in table 6, showing separately in Figure 7 the 6 last ones, with  $D_i V_j, i \neq j$  (discrete representation  $T_2^+$ ) and the 5 first ones, with  $D_i V_i$  (discrete representation  $E^+$ ) for all three masses of the  $B$  meson, for  $\beta = 3.9$  and  $\beta = 4.05$ .

As can be seen all these plots show similar shapes. There is a fair agreement between both representations of the discrete group. There is a positive noisy signal, culminating around 6 for  $\beta = 4.05$ , or even higher for heavier  $B$  masses. For  $\beta = 4.05$  ( $\beta = 3.9$ ) there are respectively 7,4,3 (2,4,5) points with a signal-to-noise ratio above 2.5 (2.) for  $B$  meson masses of 2.5, 3. and 3.7 GeV, respectively.

To conclude we may claim that *we have got a significant signal for the decay  $B \rightarrow D_2^* l \nu$  with finite  $m_{c,b}$* . The ratio over the infinite mass limit estimate is significantly larger than what we would have expected, i.e. larger than 1, but in the right order of magnitude.

## 7 Conclusions and prospects

The major goal of this paper concerned the orbitally excited states of the charmed mesons and the semileptonic decay of the  $B$  meson into the latter. We have concentrated on the  $D_2^*$  and  $D_0^*$  (see [37] for a study of the mass spectrum including the spin 1 particles). We have considered three “ $B$  mesons” with respectively masses of 2.5, 3., 3.7 GeV. We have used only two lattice spacings, 0.085 and 0.069 fm.

Concerning the spectroscopy, we have noted a discrepancy between the masses of the  $D_2^*$  states which are in the  $E$  ( $D_i V_i$ ) discrete group and the ones in the  $T_2$  ( $D_i V_j; j \neq i$ ). This is of course a lattice artefact. We have also studied the  $B$  meson energy as a function of the momentum. We have looked at the energy of the  $B$  mesons as a function of the momentum. There is a clear departure from the theoretical formula for the heaviest meson. This is presumably also an artefact. The  $D_0^*$  state can decay into a  $D$  meson due to the parity violation when using twisted quarks. It was necessary to use the GEVP method to overcome this difficulty. The mass differences between the  $D_2^*$  ( $D_0^*$ ) with the  $D$  meson mass, extrapolated to the continuum, do not agree well with experiment. A smaller lattice spacings might improve significantly this result.

To compute the form factors and branching fractions we have derived all the needed theoretical formulae necessary to estimate any form factor from lattice calculation.

Concerning  $B \rightarrow D_0^*$  we have up to now only considered the zero recoil quantity. Our result is that, contrary to the case at infinite  $b$  and  $c$  masses, the zero recoil amplitude does not vanish. This should increase drastically the  $B \rightarrow D_0^*$  branching fraction as compared to the  $B \rightarrow D_2^*$  as compared to the infinite mass case and go in the direction of solving a well known problem between experiment and the infinite mass theoretical prediction. However our extrapolation to the continuum has more than 100 % error.

The  $B \rightarrow D_2^*$  is treated by a subtraction of the zero recoil contribution which we prove to be theoretically vanishing. There is a clear signal although still rather noisy. We take the infinite mass result as a benchmark. The ratio to the

infinite mass prediction is rather large climbing up to 10 for the central value. We would have expected ratios closer to 1. We do not yet understand the reason for these large numbers.

Altogether, this paper has to be taken as a preliminary study. To our knowledge it is the first study of semileptonic decays do orbitally excited charmed mesons with finite masses for the  $b$  and  $c$ . The considered process is very noisy and it is already rewarding that we got signals which seem to make sense, although the uncertainty is really too large in the continuum limit.

To improve the situation it seems that the path to follow is to perform the same analysis with the data set of ETMC at  $\beta = 4.2$  ( $a \simeq 0.055$  fm). The extrapolation to the continuum will thus be on a much safer ground. An increase of the statistics will also help.

## Acknowledgements

## Appendix

### Coefficients of the hadronic tensor $W_{\mu\nu}$

In order to compute explicitly the coefficients  $\alpha$ ,  $\beta_{++}$ ,  $\beta_{+-}$ ,  $\beta_{-+}$ ,  $\beta_{--}$  and  $\gamma$  given in (2.3), we will have to evaluate the possible summation over the  $D^{**}$  spins.

Scalar meson : no summation and we get

$$\begin{aligned} \boxed{\alpha} &= 0 & \boxed{\gamma} &= 0 \\ \boxed{\beta_{++}} &= \tilde{u}_+^2 & \boxed{\beta_{+-}} &= \tilde{u}_+ \tilde{u}_- & \boxed{\beta_{-+}} &= \tilde{u}_+ \tilde{u}_- & \boxed{\beta_{--}} &= \tilde{u}_-^2 \end{aligned}$$

Tensor meson  $J=2$  : the polarisation tensor  $\varepsilon_{\mu\nu}^{(p)}$  satisfies [38, 39] :

$$\begin{aligned} \sum_s \varepsilon_{\mu\nu}^{(p)*} \varepsilon_{\rho\sigma}^{(p)} &= -\frac{1}{3} \left( g_{\mu\nu} - \frac{p_\mu p_\nu}{p^2} \right) \left( g_{\rho\sigma} - \frac{p_\rho p_\sigma}{p^2} \right) \\ &\quad + \frac{1}{2} \left( g_{\mu\rho} - \frac{p_\mu p_\rho}{p^2} \right) \left( g_{\nu\sigma} - \frac{p_\nu p_\sigma}{p^2} \right) + \frac{1}{2} \left( g_{\mu\sigma} - \frac{p_\mu p_\sigma}{p^2} \right) \left( g_{\nu\rho} - \frac{p_\nu p_\rho}{p^2} \right) \end{aligned}$$

After calculation, we obtain:

$$\boxed{\alpha} = -\frac{(p_B \cdot p_{D_2^*})^2 - m_B^2 m_{D_2^*}^2}{2 m_{D_2^*}^2} \left[ \tilde{k}^2 + 4 \tilde{h}^2 \left( (p_B \cdot p_{D_2^*})^2 - m_B^2 m_{D_2^*}^2 \right) \right]$$

$$\begin{aligned} \boxed{\beta_{++}} &= \frac{2 \tilde{k} \tilde{b}_+}{3 m_{D_2^*}^4} \left( p_B \cdot p_{D_2^*} - m_{D_2^*}^2 \right) \left( (p_B \cdot p_{D_2^*})^2 - m_B^2 m_{D_2^*}^2 \right) + \frac{2 \tilde{b}_+^2}{3 m_{D_2^*}^4} \left( (p_B \cdot p_{D_2^*})^2 - m_B^2 m_{D_2^*}^2 \right)^2 \\ &\quad - \frac{\tilde{h}^2}{2 m_{D_2^*}^2} \left( (p_B \cdot p_{D_2^*})^2 - m_B^2 m_{D_2^*}^2 \right) (p_B - p_{D_2^*})^2 + \frac{\tilde{k}^2}{24 m_{D_2^*}^4} \left[ m_{D_2^*}^2 (p_B - p_{D_2^*})^2 + 4 \left( (p_B \cdot p_{D_2^*})^2 - m_B^2 m_{D_2^*}^2 \right) \right] \end{aligned}$$

$$\begin{aligned} \boxed{\beta_{+-}} &= \boxed{\beta_{-+}} = \frac{2 \tilde{b}_+ \tilde{b}_-}{3 m_{D_2^*}^4} \left( (p_B \cdot p_{D_2^*})^2 - m_B^2 m_{D_2^*}^2 \right)^2 + \frac{\tilde{k} \tilde{b}_-}{3 m_{D_2^*}^4} \left( p_B \cdot p_{D_2^*} - m_{D_2^*}^2 \right) \left( (p_B \cdot p_{D_2^*})^2 - m_B^2 m_{D_2^*}^2 \right) \\ &\quad - \frac{\tilde{k} \tilde{b}_+}{3 m_{D_2^*}^4} \left( p_B \cdot p_{D_2^*} + m_{D_2^*}^2 \right) \left( (p_B \cdot p_{D_2^*})^2 - m_B^2 m_{D_2^*}^2 \right) + \frac{\tilde{h}^2}{2 m_{D_2^*}^2} (m_B^2 - m_{D_2^*}^2) \left( (p_B \cdot p_{D_2^*})^2 - m_B^2 m_{D_2^*}^2 \right) \\ &\quad + \frac{\tilde{k}^2}{24 m_{D_2^*}^4} \left( 3 m_B^2 m_{D_2^*}^2 - 4 (p_B \cdot p_{D_2^*})^2 + m_{D_2^*}^4 \right) \end{aligned}$$

$$\begin{aligned} \boxed{\beta_{--}} &= -\frac{2 \tilde{k} \tilde{b}_-}{3 m_{D_2^*}^4} \left( p_B \cdot p_{D_2^*} + m_{D_2^*}^2 \right) \left( (p_B \cdot p_{D_2^*})^2 - m_B^2 m_{D_2^*}^2 \right) + \frac{2 \tilde{b}_-^2}{3 m_{D_2^*}^4} \left( (p_B \cdot p_{D_2^*})^2 - m_B^2 m_{D_2^*}^2 \right)^2 \\ &\quad - \frac{\tilde{h}^2}{2 m_{D_2^*}^2} \left( (p_B \cdot p_{D_2^*})^2 - m_B^2 m_{D_2^*}^2 \right) (p_B + p_{D_2^*})^2 + \frac{\tilde{k}^2}{24 m_{D_2^*}^4} \left[ m_{D_2^*}^2 (p_B + p_{D_2^*})^2 + 4 \left( (p_B \cdot p_{D_2^*})^2 - m_B^2 m_{D_2^*}^2 \right) \right] \end{aligned}$$

$$\boxed{\gamma} = \frac{\tilde{k} \tilde{h}}{m_{D_2^*}^2} \left( (p_B \cdot p_{D_2^*})^2 - m_B^2 m_{D_2^*}^2 \right)$$

## Variation domains of $x$ and $y$

**First type of constraints :  $x = x(y)$**

Non-zero mass lepton :

$$(m_\ell \neq 0) \quad \left\{ \begin{array}{l} x_{\max} = \frac{1}{2} \left\{ 1 + y - r_{D^{**}}^2 + r_\ell^2 \left[ 1 + \frac{1}{y} (1 - r_{D^{**}}^2) \right] + \left( 1 - \frac{r_\ell^2}{y} \right) \sqrt{[y - (1 - r_{D^{**}})^2] [y - (1 + r_{D^{**}})^2]} \right\} \\ x_{\min} = \frac{1}{2} \left\{ 1 + y - r_{D^{**}}^2 + r_\ell^2 \left[ 1 + \frac{1}{y} (1 - r_{D^{**}}^2) \right] - \left( 1 - \frac{r_\ell^2}{y} \right) \sqrt{[y - (1 - r_{D^{**}})^2] [y - (1 + r_{D^{**}})^2]} \right\} \end{array} \right.$$

with :  $r_\ell^2 \leq y \leq (1 - r_{D^{**}})^2$

Zero mass lepton :

$$(m_\ell = 0) \quad \left\{ \begin{array}{l} x_{\max} = \frac{1}{2} \left[ 1 + y - r_{D^{**}}^2 + \sqrt{[y - (1 - r_{D^{**}})^2] [y - (1 + r_{D^{**}})^2]} \right] \\ x_{\min} = \frac{1}{2} \left[ 1 + y - r_{D^{**}}^2 - \sqrt{[y - (1 - r_{D^{**}})^2] [y - (1 + r_{D^{**}})^2]} \right] \end{array} \right.$$

with :  $0 \leq y \leq (1 - r_{D^{**}})^2$

**Second type of constraints :  $y = y(x)$**

Non-zero mass lepton :

$$(m_\ell \neq 0) \quad \left\{ \begin{array}{l} y_{\max} = \frac{1}{2} \left[ x - \frac{r_{D^{**}}^2 (x - 2r_\ell^2)}{1 - x + r_\ell^2} + \left( 1 - \frac{r_{D^{**}}^2}{1 - x + r_\ell^2} \right) \sqrt{x^2 - 4r_\ell^2} \right] \\ y_{\min} = \frac{1}{2} \left[ x - \frac{r_{D^{**}}^2 (x - 2r_\ell^2)}{1 - x + r_\ell^2} - \left( 1 - \frac{r_{D^{**}}^2}{1 - x + r_\ell^2} \right) \sqrt{x^2 - 4r_\ell^2} \right] \end{array} \right.$$

with :  $2r_\ell \leq x \leq 1 - r_{D^{**}}^2 + r_\ell^2$

Zero mass lepton :

$$(m_\ell = 0) \quad \left\{ \begin{array}{l} y_{\max} = x \left( 1 - \frac{r_{D^{**}}^2}{1 - x} \right) \\ y_{\min} = 0 \end{array} \right.$$

with :  $0 \leq x \leq 1 - r_{D^{**}}^2$

## Expressions for the various decay widths

$\frac{d^2\Gamma}{dx dy}$  differential decay width

►  $\boxed{{}^3P_0 \text{ states}}$  :

Non-zero mass lepton :

$$\frac{d^2\Gamma}{dx dy} = -\frac{G_F^2 |V_{cb}|^2}{128\pi^3} m_B^5 \left\{ -\tilde{u}_+^2 \left[ 4 \left[ x r_{D_0^*}^2 + (1 - x)(y - x) \right] + r_\ell^2 \left[ 3y - 4(x + r_{D_0^*}^2) + r_\ell^2 \right] \right] \right. \\ \left. + 2 \tilde{u}_+ \tilde{u}_- r_\ell^2 \left[ 2(1 - x - r_{D_0^*}^2) + y + r_\ell^2 \right] \right. \\ \left. + \tilde{u}_-^2 r_\ell^2 (y - r_\ell^2) \right\}$$

Zero mass lepton :

$$\frac{d^2\Gamma}{dx dy} = \frac{G_F^2 |V_{cb}|^2}{32\pi^3} m_B^5 \tilde{u}_+^2 \left[ x r_{D_0^*}^2 + (1 - x)(y - x) \right]$$

►  $^3P_2$  states :

Non-zero mass lepton :

$$\frac{d^2\Gamma}{dx dy} = -\frac{m_B}{256\pi^3} \frac{G_F^2 |V_{cb}|^2}{2} \left\{ C_1 \tilde{k}^2 + C_2 \tilde{h}^2 + C_3 \tilde{b}_+^2 + C_4 \tilde{b}_-^2 + 2 C_5 \tilde{k} \tilde{b}_+ + 2 C_6 \tilde{k} \tilde{b}_- + 2 C_7 \tilde{b}_+ \tilde{b}_- + 2 C_8 \tilde{h} \tilde{k} \right\}$$

where the  $C_i$  coefficients are given by :

$$C_1 = \frac{m_B^4}{3 r_{D_2^*}^4} \left\{ \left[ y^2 - (2 + r_{D_2^*}^2) y + (1 - r_{D_2^*}^2)^2 \right] \left[ 2(1-x)(x-y) + r_{D_2^*}^2 (3y-2x) \right] - 3 y^2 r_{D_2^*}^4 \right. \\ \left. - r_\ell^2 \left[ (1-2x+y) \left[ 2(1-y)^2 - 3 r_{D_2^*}^2 (1+y) \right] - r_{D_2^*}^4 (2x - r_{D_2^*}^2) \right] \right. \\ \left. - 2 r_\ell^4 \left[ y^2 - 2(1 + r_{D_2^*}^2) y + 1 - r_{D_2^*}^2 + r_{D_2^*}^4 \right] \right\}$$

$$C_2 = \frac{m_B^8}{r_{D_2^*}^2} \left[ y - (1 - r_{D_2^*}^2)^2 \right] \left[ y - (1 + r_{D_2^*}^2)^2 \right] \\ \times \left[ y \left[ 2(1-x+r_{D_2^*}^2)(1-x-r_{D_2^*}^2) - (1-y+r_{D_2^*}^2)(1+y-2x-r_{D_2^*}^2) \right] \right. \\ \left. + r_\ell^2 \left[ (1+y-r_{D_2^*}^2)(1+y-2x-r_{D_2^*}^2) + 2 r_\ell^2 \right] \right]$$

$$C_3 = \frac{m_B^8}{6 r_{D_2^*}^4} \left[ y - (1 - r_{D_2^*}^2)^2 \right]^2 \left[ y - (1 + r_{D_2^*}^2)^2 \right]^2 \left[ 4x(1-x-r_{D_2^*}^2) - 4y(1-x) + r_\ell^2 \left[ 4(x+r_{D_2^*}^2) - 3y - r_\ell^2 \right] \right]$$

$$C_4 = \frac{m_B^8}{6 r_{D_2^*}^4} r_\ell^2 (y - r_\ell^2) \left[ y - (1 - r_{D_2^*}^2)^2 \right]^2 \left[ y - (1 + r_{D_2^*}^2)^2 \right]^2$$

$$C_5 = \frac{m_B^6}{3 r_{D_2^*}^4} \left[ y - (1 - r_{D_2^*}^2)^2 \right] \left[ y - (1 + r_{D_2^*}^2)^2 \right] \\ \times \left[ 2(1-y-r_{D_2^*}^2) \left[ (1-x)(x-y) - x r_{D_2^*}^2 \right] - r_\ell^2 \left[ (1-y+r_{D_2^*}^2)(1-3x+2y-r_{D_2^*}^2+r_\ell^2) + 2x r_{D_2^*}^2 \right] \right]$$

$$C_6 = \frac{m_B^6}{3 r_{D_2^*}^4} r_\ell^2 \left[ y - (1 - r_{D_2^*}^2)^2 \right] \left[ y - (1 + r_{D_2^*}^2)^2 \right] \\ \times \left[ (1-y+r_{D_2^*}^2)(1-x+r_{D_2^*}^2) + 2 r_{D_2^*}^2 (x-2) + r_\ell^2 (1-y+r_{D_2^*}^2) \right]$$

$$C_7 = \frac{m_B^8}{6 r_{D_2^*}^4} r_\ell^2 \left[ y - (1 - r_{D_2^*}^2)^2 \right]^2 \left[ y - (1 + r_{D_2^*}^2)^2 \right]^2 \left[ 2(1-x-r_{D_2^*}^2) + y + r_\ell^2 \right]$$

$$C_8 = -\frac{m_B^6}{r_{D_2^*}^2} \left[ y - (1 - r_{D_2^*}^2)^2 \right] \left[ y - (1 + r_{D_2^*}^2)^2 \right] \left[ y(1+y-2x-r_{D_2^*}^2) + r_\ell^2 (1+y-r_{D_2^*}^2) \right]$$

Zero mass lepton : We notice that the coefficients of  $C_4$ ,  $C_6$  and  $C_7$  cancel in this limit, leading to :

$$\frac{d^2\Gamma}{dx dy} = -\frac{m_B}{256\pi^3} \frac{G_F^2 |V_{cb}|^2}{2} \left[ C_1 \tilde{k}^2 + C_2 \tilde{h}^2 + C_3 \tilde{b}_+^2 + 2 C_5 \tilde{k} \tilde{b}_+ + 2 C_8 \tilde{h} \tilde{k} \right]$$

where the  $C_i$  coefficients are given by :

$$C_1 = \frac{m_B^4}{3 r_{D_2^*}^4} \left[ \left[ y^2 - (2 + r_{D_2^*}^2) y + (1 - r_{D_2^*}^2)^2 \right] \left[ 2(1-x)(x-y) + r_{D_2^*}^2 (3y-2x) \right] - 3y^2 r_{D_2^*}^4 \right]$$

$$C_2 = \frac{m_B^8}{r_{D_2^*}^2} \left[ y - (1 - r_{D_2^*}^2)^2 \right] \left[ y - (1 + r_{D_2^*}^2)^2 \right] \\ \times y \left[ 2(1-x+r_{D_2^*}^2)(1-x-r_{D_2^*}^2) - (1-y+r_{D_2^*}^2)(1+y-2x-r_{D_2^*}^2) \right]$$

$$C_3 = \frac{m_B^8}{6 r_{D_2^*}^4} \left[ y - (1 - r_{D_2^*}^2)^2 \right]^2 \left[ y - (1 + r_{D_2^*}^2)^2 \right]^2 \left[ 4x(1-x-r_{D_2^*}^2) - 4y(1-x) \right]$$

$$C_5 = \frac{m_B^6}{3 r_{D_2^*}^4} \left[ y - (1 - r_{D_2^*}^2)^2 \right] \left[ y - (1 + r_{D_2^*}^2)^2 \right] \left[ 2(1-y-r_{D_2^*}^2) \left[ (1-x)(x-y) - x r_{D_2^*}^2 \right] \right]$$

$$C_8 = -\frac{m_B^6}{r_{D_2^*}^2} \left[ y - (1 - r_{D_2^*}^2)^2 \right] \left[ y - (1 + r_{D_2^*}^2)^2 \right] y (1+y-2x-r_{D_2^*}^2)$$

$\frac{d\Gamma}{dy}$  **differential decay width**

The form factors depend only on the  $y$  parameter, but in an unknown way. So, the integration over the  $x$  variable can be done through the use the expressions of the type  $x = x(y)$ .

►  $^3P_0$  states :

Non-zero mass lepton :

$$\frac{d\Gamma}{dy} = -\frac{G_F^2 |V_{cb}|^2}{128\pi^3} m_B^5 \left[ D_1 \tilde{u}_+^2 + 2 D_2 \tilde{u}_+ \tilde{u}_- + D_3 \tilde{u}_-^2 \right]$$

where the  $D_i$  coefficients are function of  $y$  and are given by :

$$D_1 = \frac{1}{3y^3} (y-r_\ell^2)^2 \left[ \left[ y - (1 - r_{D_0^*}^2) \right] \left[ y - (1 + r_{D_0^*}^2) \right] \right]^{1/2} \\ \times \left\{ 2y \left[ y - (1 - r_{D_0^*}^2) \right] \left[ y - (1 + r_{D_0^*}^2) \right] + r_\ell^2 \left[ y^2 - 2y(1+r_{D_0^*}^2) + 4(1-r_{D_0^*}^2)^2 \right] \right\}$$

$$D_2 = \frac{1}{y^2} r_\ell^2 (y-r_\ell^2)^2 (1-r_{D_0^*}^2) \left[ \left[ y - (1 - r_{D_0^*}^2) \right] \left[ y - (1 + r_{D_0^*}^2) \right] \right]^{1/2}$$

$$D_3 = \frac{1}{y} r_\ell^2 (y-r_\ell^2)^2 \left[ \left[ y - (1 - r_{D_0^*}^2) \right] \left[ y - (1 + r_{D_0^*}^2) \right] \right]^{1/2}$$

Let us recall that, in that expression of  $d\Gamma/dy$ , the  $y$  parameter belongs in the interval :  $r_\ell^2 \leq y \leq (1 - r_{D_0^*}^2)^2$

Zero mass lepton :

$$\frac{d\Gamma}{dy} = -\frac{G_F^2 |V_{cb}|^2}{128\pi^3} m_B^5 \tilde{u}_+^2 D_1 \quad \text{where} \quad D_1 = \frac{2}{3} \left[ \left[ y - (1 - r_{D_0^*}^2) \right] \left[ y - (1 + r_{D_0^*}^2) \right] \right]^{3/2}$$

since the other coefficients  $D_2$  and  $D_3$  give zero in this case.

►  $^3P_2$  states :

Non-zero mass lepton :

$$\frac{d\Gamma}{dy} = -\frac{m_B}{256\pi^3} \frac{G_F^2 |V_{cb}|^2}{2} \left\{ D_1 \tilde{k}^2 + D_2 \tilde{h}^2 + D_3 \tilde{b}_+^2 + D_4 \tilde{b}_-^2 + 2 D_5 \tilde{k} \tilde{b}_+ + 2 D_6 \tilde{k} \tilde{b}_- + 2 D_7 \tilde{b}_+ \tilde{b}_- + 2 D_8 \tilde{h} \tilde{k} \right\}$$

where the  $D_i$  coefficients are given by :

$$D_1 = \frac{m_B^4}{r_{D_2^*}^4} \frac{1}{9y^3} (y - r_\ell^2)^2 \left[ [y - (1 - r_{D_2^*})^2] [y - (1 + r_{D_2^*})^2] \right]^{3/2} \\ \times \left\{ y [y^2 - 2y(1 - 4r_{D_2^*}^2) + (1 - r_{D_2^*}^2)^2] + r_\ell^2 [2y^2 - y(4 - r_{D_2^*}^2) + 2(1 - r_{D_2^*}^2)^2] \right\}$$

$$D_2 = \frac{m_B^8}{r_{D_2^*}^2} \frac{1}{3y^2} (y - r_\ell^2)^2 (2y + r_\ell^2) \left[ [y - (1 - r_{D_2^*})^2] [y - (1 + r_{D_2^*})^2] \right]^{5/2}$$

$$D_3 = \frac{m_B^8}{r_{D_2^*}^4} \frac{1}{18y^3} (y - r_\ell^2)^2 \left[ [y - (1 - r_{D_2^*})^2] [y - (1 + r_{D_2^*})^2] \right]^{5/2} \\ \times \left\{ 2y [y - (1 - r_{D_2^*})^2] [y - (1 + r_{D_2^*})^2] + r_\ell^2 [y^2 - 2y(1 + r_{D_2^*}^2) + 4(1 - r_{D_2^*}^2)^2] \right\}$$

$$D_4 = \frac{m_B^8}{r_{D_2^*}^4} \frac{1}{6y} r_\ell^2 (y - r_\ell^2)^2 \left[ [y - (1 - r_{D_2^*})^2] [y - (1 + r_{D_2^*})^2] \right]^{5/2}$$

$$D_5 = \frac{m_B^6}{r_{D_2^*}^4} \frac{1}{18y^3} (y - r_\ell^2)^2 \left[ [y - (1 - r_{D_2^*})^2] [y - (1 + r_{D_2^*})^2] \right]^{5/2} \left[ 2y(1 - y - r_{D_2^*}^2) + r_\ell^2(4 - y - 4r_{D_2^*}^2) \right]$$

$$D_6 = \frac{m_B^6}{r_{D_2^*}^4} \frac{1}{6y^2} r_\ell^2 (y - r_\ell^2)^2 \left[ [y - (1 - r_{D_2^*})^2] [y - (1 + r_{D_2^*})^2] \right]^{5/2}$$

$$D_7 = \frac{m_B^8}{r_{D_2^*}^4} \frac{1}{6y^2} r_\ell^2 (y - r_\ell^2)^2 (1 - r_{D_2^*}^2) \left[ [y - (1 - r_{D_2^*})^2] [y - (1 + r_{D_2^*})^2] \right]^{5/2}$$

$$D_8 = 0$$

We recall that, in those formulae, the  $y$  parameter varies inside the domain :  $r_\ell^2 \leq y \leq (1 - r_{D_2^*})^2$

Zero mass lepton :

$$\frac{d\Gamma}{dy} = -\frac{m_B}{256\pi^3} \frac{G_F^2 |V_{cb}|^2}{2} \left[ D_1 \tilde{k}^2 + D_2 \tilde{h}^2 + D_3 \tilde{b}_+^2 + 2 D_5 \tilde{k} \tilde{b}_+ + 2 D_8 \tilde{h} \tilde{k} \right]$$

where the  $D_i$  coefficients are given by :

$$D_1 = \frac{m_B^4}{r_{D_2^*}^4} \frac{1}{9} \left[ [y - (1 - r_{D_2^*})^2] [y - (1 + r_{D_2^*})^2] \right]^{3/2} [y^2 - 2y(1 - 4r_{D_2^*}^2) + (1 - r_{D_2^*}^2)^2]$$

$$D_2 = \frac{m_B^8}{r_{D_2^*}^2} \frac{2}{3} y \left[ [y - (1 - r_{D_2^*})^2] [y - (1 + r_{D_2^*})^2] \right]^{5/2}$$

$$D_3 = \frac{m_B^8}{r_{D_2^*}^4} \frac{1}{9} \left[ \left[ y - (1 - r_{D_2^*})^2 \right] \left[ y - (1 + r_{D_2^*})^2 \right] \right]^{7/2}$$

$$D_5 = \frac{m_B^6}{r_{D_2^*}^4} \frac{1}{9} (1 - y - r_{D_2^*}^2) \left[ \left[ y - (1 - r_{D_2^*})^2 \right] \left[ y - (1 + r_{D_2^*})^2 \right] \right]^{5/2}$$

$$D_8 = 0$$

Here, the  $y$  parameter lies in the domain :  $0 \leq y \leq (1 - r_{D_2^*})^2$

### $\frac{d\Gamma}{dx}$ differential decay width

It is impossible to give general expressions for the leptonic spectra  $\frac{d\Gamma}{dx}$  since the integration over  $y$  can not be performed because we do not know the dependance of the form factors on  $y$ .

Nevertheless, the procedure to do those calculations is the following :

1. We start from the expressions of the  $\frac{d^2\Gamma}{dx dy}$  decay widths given above
2. We use the constraints of the type  $y = y(x)$  in order to perform the integration over  $y$  from  $y_{\min}$  to  $y_{\max}$  (expressions given also above). Incidentally, we must not forget that the maximum of  $E_{D^{**}}$  corresponds to the minimum of  $y$  and vice-versa. So, to integrate over  $E_{D^{**}}$  from  $E_{D^{**}}^{\min}$  to  $E_{D^{**}}^{\max}$ , we have to integrate equivalently over  $y$  from  $y_{\max}$  to  $y_{\min}$  :

$$\frac{d\Gamma}{dx} = \int_{y_{\max}}^{y_{\min}} \frac{d^2\Gamma}{dx dy} dy$$

with :

$$\begin{cases} y_{\max} = \frac{1}{2} \left[ x - \frac{r_{D^{**}}^2 (x - 2r_\ell^2)}{1 - x + r_\ell^2} + \left( 1 - \frac{r_{D^{**}}^2}{1 - x + r_\ell^2} \right) \sqrt{x^2 - 4r_\ell^2} \right] \\ y_{\min} = \frac{1}{2} \left[ x - \frac{r_{D^{**}}^2 (x - 2r_\ell^2)}{1 - x + r_\ell^2} - \left( 1 - \frac{r_{D^{**}}^2}{1 - x + r_\ell^2} \right) \sqrt{x^2 - 4r_\ell^2} \right] \end{cases}$$

( $r_\ell = 0$  gives the relations in the case of a zero mass lepton.)

3. The last free parameter  $x$  lies in the domain :

$$2r_\ell \leq x \leq 1 - r_{D^{**}}^2 + r_\ell^2$$

(Once again,  $r_\ell = 0$  gives the variation domain in the case of a zero mass lepton.)

### Total decay width $\Gamma$

The problem, mentioned for the leptonic spectra, pops up here again because, in order to get  $\Gamma$ , we will have to integrate over  $y$  at some point. So we will have to follow the same procedure.

### Polarization tensor for the $^3P_2$ state

Using expressions for the spin-1 polarisation vector found in [40] for instance and the values of the Clebsch-Gordan coefficient from the “Particle Physics Booklet”, we get :

$$\begin{aligned} \varepsilon_{(+2)}^{\mu\nu} &= \frac{1}{2} \begin{pmatrix} 0 & 0 & 0 & 0 \\ 0 & 1 & i & 0 \\ 0 & i & -1 & 0 \\ 0 & 0 & 0 & 0 \end{pmatrix} & \varepsilon_{(-2)}^{\mu\nu} &= \frac{1}{2} \begin{pmatrix} 0 & 0 & 0 & 0 \\ 0 & 1 & -i & 0 \\ 0 & -i & -1 & 0 \\ 0 & 0 & 0 & 0 \end{pmatrix} & \varepsilon_{(+1)}^{\mu\nu} &= \frac{1}{2} \begin{pmatrix} 0 & 0 & 0 & 0 \\ 0 & 0 & 0 & -1 \\ 0 & 0 & 0 & -i \\ 0 & -1 & -i & 0 \end{pmatrix} \\ \varepsilon_{(-1)}^{\mu\nu} &= \frac{1}{2} \begin{pmatrix} 0 & 0 & 0 & 0 \\ 0 & 0 & 0 & 1 \\ 0 & 0 & 0 & -i \\ 0 & 1 & -i & 0 \end{pmatrix} & \varepsilon_{(0)}^{\mu\nu} &= \frac{1}{\sqrt{6}} \begin{pmatrix} 0 & 0 & 0 & 0 \\ 0 & -1 & 0 & 0 \\ 0 & 0 & -1 & 0 \\ 0 & 0 & 0 & 2 \end{pmatrix} \end{aligned}$$

(We dropped the  $\vec{0}$  in the notation.)



## Extraction of the form factors

The following expressions are not exhaustive.

Note that it is possible to recover the momentum transfer  $y m_B^2 = (p_B - p_{D^{**}})^2$  using :

$$E_B = \frac{m_B}{2 r_{D^{**}}} [1 - y + r_{D^{**}}^2] \quad \text{and} \quad p^2 = \frac{m_B^2}{12 r_{D^{**}}^2} [y - (1 - r_{D^{**}})^2] [y - (1 + r_{D^{**}})^2]$$

leading to :

$$E_B + m_{D^{**}} = \frac{m_B}{2 r_{D^{**}}} (1 - y + 3 r_{D^{**}}^2) \quad E_B - m_{D^{**}} = \frac{m_B}{2 r_{D^{**}}} (1 - y - r_{D^{**}}^2)$$

### ${}^3P_0$ form factors

With  $\mathcal{T}_\mu^A \stackrel{\text{def.}}{=} \langle {}^3P_0 | A_\mu | B(p_B) \rangle$

- form factor  $\tilde{u}_+$  :

$$\boxed{\tilde{u}_+} = -\frac{1}{2 m_{D^{**}}} \left[ \frac{E_B - m_{D^{**}}}{p} \mathcal{T}_i^A - \mathcal{T}_0^A \right] = -\frac{1}{2 m_{D^{**}}} \left[ \frac{E_B - m_{D^{**}}}{3 p} (\mathcal{T}_1^A + \mathcal{T}_2^A + \mathcal{T}_3^A) - \mathcal{T}_0^A \right]$$

- form factor  $\tilde{u}_-$  :

$$\boxed{\tilde{u}_-} = \frac{1}{2 m_{D^{**}}} \left[ \frac{E_B + m_{D^{**}}}{p} \mathcal{T}_i^A - \mathcal{T}_0^A \right] = \frac{1}{2 m_{D^{**}}} \left[ \frac{E_B + m_{D^{**}}}{3 p} (\mathcal{T}_1^A + \mathcal{T}_2^A + \mathcal{T}_3^A) - \mathcal{T}_0^A \right]$$

### ${}^3P_2$ form factors

With  $\mathcal{T}_{\mu(\lambda)}^A \stackrel{\text{def.}}{=} \langle {}^3P_2(\lambda) | A_\mu | B(p_B) \rangle$  and  $\mathcal{T}_{\mu(\lambda)}^V \stackrel{\text{def.}}{=} \langle {}^3P_2(\lambda) | V_\mu | B(p_B) \rangle$

- form factor  $\tilde{k}$  :

$$\boxed{\tilde{k}} = -\frac{\sqrt{6}}{p} \mathcal{T}_{1(0)}^A = -\frac{\sqrt{6}}{p} \mathcal{T}_{2(0)}^A = \frac{\sqrt{6}}{2 p} \mathcal{T}_{3(0)}^A = \frac{1}{p} [\mathcal{T}_{1(+2)}^A + \mathcal{T}_{1(-2)}^A] = -\frac{1}{p} [\mathcal{T}_{2(+2)}^A + \mathcal{T}_{2(-2)}^A]$$

- form factors  $\tilde{b}_+$  and  $\tilde{b}_-$  :

$$\begin{aligned} & \left\{ \begin{aligned} \boxed{\tilde{b}_+} &= -\frac{1+i}{4} \frac{1}{p^3 m_{D^{**}}} [(E_B - m_{D^{**}})(i \mathcal{T}_{1(+2)}^A + \mathcal{T}_{2(+2)}^A) - p(1+i) \mathcal{T}_{0(+2)}^A] \\ \boxed{\tilde{b}_-} &= \frac{1+i}{4} \frac{1}{p^3 m_{D^{**}}} [(E_B + m_{D^{**}})(i \mathcal{T}_{1(+2)}^A + \mathcal{T}_{2(+2)}^A) - p(1+i) \mathcal{T}_{0(+2)}^A] \end{aligned} \right. \\ & \left\{ \begin{aligned} \boxed{\tilde{b}_+} &= \frac{1-i}{4} \frac{1}{p^3 m_{D^{**}}} [(E_B - m_{D^{**}})(i \mathcal{T}_{1(-2)}^A - \mathcal{T}_{2(-2)}^A) + p(1-i) \mathcal{T}_{0(-2)}^A] \\ \boxed{\tilde{b}_-} &= -\frac{1-i}{4} \frac{1}{p^3 m_{D^{**}}} [(E_B + m_{D^{**}})(i \mathcal{T}_{1(-2)}^A - \mathcal{T}_{2(-2)}^A) + p(1-i) \mathcal{T}_{0(-2)}^A] \end{aligned} \right. \\ & \left\{ \begin{aligned} \boxed{\tilde{b}_+} &= \frac{1+i}{4} \frac{1}{p^3 m_{D^{**}}} [(E_B - m_{D^{**}})(\mathcal{T}_{1(+1)}^A + \mathcal{T}_{2(+1)}^A - \mathcal{T}_{3(+1)}^A) - p \mathcal{T}_{0(+1)}^A] \\ \boxed{\tilde{b}_-} &= -\frac{1+i}{4} \frac{1}{p^3 m_{D^{**}}} [(E_B + m_{D^{**}})(\mathcal{T}_{1(+1)}^A + \mathcal{T}_{2(+1)}^A - \mathcal{T}_{3(+1)}^A) - p \mathcal{T}_{0(+1)}^A] \end{aligned} \right. \\ & \left\{ \begin{aligned} \boxed{\tilde{b}_+} &= -\frac{1-i}{4} \frac{1}{p^3 m_{D^{**}}} [(E_B - m_{D^{**}})(\mathcal{T}_{1(-1)}^A + \mathcal{T}_{2(-1)}^A - \mathcal{T}_{3(-1)}^A) - p \mathcal{T}_{0(-1)}^A] \\ \boxed{\tilde{b}_-} &= \frac{1-i}{4} \frac{1}{p^3 m_{D^{**}}} [(E_B + m_{D^{**}})(\mathcal{T}_{1(-1)}^A + \mathcal{T}_{2(-1)}^A - \mathcal{T}_{3(-1)}^A) - p \mathcal{T}_{0(-1)}^A] \end{aligned} \right. \\ & \left\{ \begin{aligned} \boxed{\tilde{b}_+} &= \frac{1}{2i} \frac{1}{p^3 m_{D^{**}}} [(E_B - m_{D^{**}}) \mathcal{T}_{3(+2)}^A - p \mathcal{T}_{0(+2)}^A] \\ \boxed{\tilde{b}_-} &= \frac{1}{2i} \frac{1}{p^3 m_{D^{**}}} [-(E_B + m_{D^{**}}) \mathcal{T}_{3(+2)}^A + p \mathcal{T}_{0(+2)}^A] \end{aligned} \right. \end{aligned}$$

- form factor  $\tilde{h}$  :

$$\boxed{\tilde{h}} = \frac{1}{2i} \frac{1}{p m_{D^{**}}} \frac{\mathcal{T}_{1(\lambda)}^V}{\varepsilon_{(\lambda)}^{*3\alpha} p_{B\alpha} - \varepsilon_{(\lambda)}^{*2\alpha} p_{B\alpha}} = \frac{1}{2i} \frac{1}{p m_{D^{**}}} \frac{\mathcal{T}_{2(\lambda)}^V}{\varepsilon_{(\lambda)}^{*1\alpha} p_{B\alpha} - \varepsilon_{(\lambda)}^{*3\alpha} p_{B\alpha}} = -\frac{1}{2i} \frac{1}{p m_{D^{**}}} \frac{\mathcal{T}_{3(\lambda)}^V}{\varepsilon_{(\lambda)}^{*2\alpha} p_{B\alpha} - \varepsilon_{(\lambda)}^{*1\alpha} p_{B\alpha}}$$

where

$\lambda$	$\varepsilon_{(\lambda)}^{*3\alpha} p_{B\alpha} - \varepsilon_{(\lambda)}^{*2\alpha} p_{B\alpha}$	$\varepsilon_{(\lambda)}^{*1\alpha} p_{B\alpha} - \varepsilon_{(\lambda)}^{*3\alpha} p_{B\alpha}$	$\varepsilon_{(\lambda)}^{*2\alpha} p_{B\alpha} - \varepsilon_{(\lambda)}^{*1\alpha} p_{B\alpha}$
+2	$-\frac{p}{2}(1+i)$	$-\frac{p}{2}(1-i)$	$p$
+1	$\frac{p}{2}$	$i\frac{p}{2}$	$-\frac{p}{2}(1+i)$
0	$-p\sqrt{\frac{3}{2}}$	$p\sqrt{\frac{3}{2}}$	0
-1	$-\frac{p}{2}$	$i\frac{p}{2}$	$\frac{p}{2}(1-i)$
-2	$-\frac{p}{2}(1-i)$	$-\frac{p}{2}(1+i)$	$p$

## Masses and energies

We collect in Table 7 the masses and energies that we extract in our analysis.

meson	$\beta = 3.9$		$\beta = 4.05$	
	$\theta$	$E(\theta)$	$\theta$	$E(\theta)$
$D$	0	0.75(1)	0	0.62(1)
$D_0^*$	0	0.96(2)	0	0.76(2)
$D_2^*$	0	1.14(2)	0	0.93(2)
$B(\mu_{h_1})$	0	1.00(1)	0	0.82(1)
$B(\mu_{h_2})$	0	1.21(1)	0	1.01(1)
$B(\mu_{h_3})$	0	1.50(1)	0	1.25(1)
$B(\mu_{h_1})$	0.99	1.02(1)	1.09	0.84(1)
$B(\mu_{h_2})$	1.21	1.24(1)	1.35	1.02(1)
$B(\mu_{h_3})$	1.48	1.51(1)	1.67	1.26(1)
$B(\mu_{h_1})$	1.41	1.04(1)	1.56	0.85(1)
$B(\mu_{h_2})$	1.72	1.26(1)	1.92	1.04(1)
$B(\mu_{h_3})$	2.11	1.52(1)	2.37	1.28(1)
$B(\mu_{h_1})$	2.02	1.08(1)	2.23	0.89(1)
$B(\mu_{h_2})$	2.46	1.30(1)	2.74	1.08(1)
$B(\mu_{h_3})$	3.01	1.55(1)	3.39	1.31(1)
$B(\mu_{h_1})$	2.50	1.12(1)	2.76	0.92(2)
$B(\mu_{h_2})$	3.05	1.34(1)	3.40	1.11(2)
$B(\mu_{h_3})$	3.73	1.58(1)	4.21	1.34(1)
$B(\mu_{h_1})$	2.92	1.16(1)	3.23	0.95(2)
$B(\mu_{h_2})$	3.56	1.38(1)	3.97	1.15(2)
$B(\mu_{h_3})$	4.36	1.60(2)	4.91	1.38(2)
$B(\mu_{h_1})$	3.66	1.25(1)	4.04	1.00(3)
$B(\mu_{h_2})$	4.46	1.46(1)	4.97	1.22(3)
$B(\mu_{h_3})$	5.46	1.66(2)	6.15	1.45(1)

Table 7: Masses and energies extracted from the two-point correlation functions in units of the lattice spacing. At  $\beta = 3.9$ , time intervals for the fits are [8, 23] ( $D$ ), [6, 9] ( $D_0^*$  and  $D_2^*$ ), [11, 17] (small momenta,  $B(\mu_{h_1})$  and  $B(\mu_{h_2})$ ), [9, 15] (large momenta,  $B(\mu_{h_1})$  and  $B(\mu_{h_2})$ ) and [9, 13] ( $B(\mu_{h_3})$ ). At  $\beta = 4.05$ , time ranges for the fits are [10, 26] ( $D$ ), [14, 26] (small momenta,  $B(\mu_{h_1})$  and  $B(\mu_{h_2})$ ), [9, 26] (large momenta,  $B(\mu_{h_1})$  and  $B(\mu_{h_2})$ ), [14, 22] (small momenta,  $B(\mu_{h_3})$ ) and [9, 22] (large momenta,  $B(\mu_{h_3})$ ).

## References

- [1] J. Beringer *et al.* [Particle Data Group Collaboration], “Review of Particle Physics (RPP)”, Phys. Rev. D **86** (2012) 010001.
- [2] P. Gambino, T. Mannel and N. Uraltsev, “ $B \rightarrow D^*$  Zero-Recoil Formfactor and the Heavy Quark Expansion in QCD: A Systematic Study”, JHEP **1210** (2012) 169 [arXiv:1206.2296 [hep-ph]].
- [3] I. I. Bigi, B. Blossier, A. Le Yaouanc, L. Oliver, O. Pene, J. -C. Raynal, A. Oyanguren and P. Roudeau, “Memorino on the ‘1/2 vs. 3/2 Puzzle’ in  $\bar{B} \rightarrow \ell \bar{\nu} X(c)$ : A Year Later and a Bit Wiser”, Eur. Phys. J. C **52** (2007) 975 [arXiv:0708.1621 [hep-ph]].
- [4] P. del Amo Sanchez *et al.* [BaBar Collaboration], “Observation of new resonances decaying to  $D\pi$  and  $D^*\pi$  in inclusive  $e^+e^-$  collisions near  $\sqrt{s}=10.58$  GeV”, Phys. Rev. D **82** (2010) 111101 [arXiv:1009.2076 [hep-ex]].
- [5] A. Le Yaouanc, L. Oliver, O. Pene and J. C. Raynal, “New heavy quark limit sum rules involving Isgur-Wise functions and decay constants”, Phys. Lett. B **387** (1996) 582 [hep-ph/9607300].
- [6] N. Uraltsev, “New exact heavy quark sum rules”, Phys. Lett. B **501** (2001) 86 [hep-ph/0011124].
- [7] V. Morenas, A. Le Yaouanc, L. Oliver, O. Pene and J. C. Raynal, “Quantitative predictions for  $B$  semileptonic decays into  $D$ ,  $D^*$  and the orbitally excited  $D^{**}$  in quark models a la Bakamjian-Thomas”, Phys. Rev. D **56** (1997) 5668 [hep-ph/9706265].
- [8] D. Ebert, R. N. Faustov and V. O. Galkin, “Exclusive semileptonic decays of  $B$  mesons to orbitally excited  $D$  mesons in the relativistic quark model”, Phys. Lett. B **434**, 365 (1998) [arXiv:hep-ph/9805423].
- [9] D. Ebert, R. N. Faustov and V. O. Galkin, “Heavy quark  $1/m_Q$  contributions in semileptonic  $B$  decays to orbitally excited  $D$  mesons”, Phys. Rev. D **61** (2000) 014016 [hep-ph/9906415].
- [10] D. Becirevic, B. Blossier, P. Boucaud, G. Herdoiza, J. P. Leroy, A. Le Yaouanc, V. Morenas and O. Pene, “Lattice measurement of the Isgur-Wise functions  $\tau_{1/2}$  and  $\tau_{3/2}$ ”, Phys. Lett. B **609** (2005) 298 [hep-lat/0406031].
- [11] B. Blossier *et al.* [European Twisted Mass Collaboration], “Lattice calculation of the Isgur-Wise functions  $\tau_{1/2}$  and  $\tau_{3/2}$  with dynamical quarks”, JHEP **0906** (2009) 022 [arXiv:0903.2298 [hep-lat]].
- [12] N. Isgur, D. Scora, B. Grinstein and M. B. Wise, “Semileptonic  $B$  and  $D$  Decays in the Quark Model”, Phys. Rev. D **39** (1989) 799.
- [13] N. Isgur and M. B. Wise, “Excited charm mesons in semileptonic  $\bar{B}$  decay and their contributions to a Bjorken sum rule”, Phys. Rev. D **43** (1991) 819.
- [14] P. Boucaud *et al.* [ETM Collaboration], “Dynamical twisted mass fermions with light quarks”, Phys. Lett. B **650** (2007) 304 [hep-lat/0701012].
- [15] C. Urbach [European Twisted Mass Collaboration], “Lattice QCD with two light Wilson quarks and maximally twisted mass”, PoS LAT **2007** (2007) 022 [arXiv:0710.1517 [hep-lat]].
- [16] P. Boucaud *et al.* [ETM Collaboration], “Dynamical Twisted Mass Fermions with Light Quarks: Simulation and Analysis Details”, Comput. Phys. Commun. **179** (2008) 695 [arXiv:0803.0224 [hep-lat]].
- [17] B. Blossier *et al.* [ETM Collaboration], “Average up/down, strange and charm quark masses with  $N_f = 2$  twisted mass lattice QCD”, Phys. Rev. D **82** (2010) 114513 [arXiv:1010.3659 [hep-lat]].
- [18] B. Blossier *et al.* [ETM Collaboration], “Ghost-gluon coupling, power corrections and  $\Lambda_{\overline{\text{MS}}}$  from twisted-mass lattice QCD at  $N_f = 2$ ”, Phys. Rev. D **82** (2010) 034510 [arXiv:1005.5290 [hep-lat]].
- [19] P. Weisz, “Continuum Limit Improved Lattice Action for Pure Yang-Mills Theory. 1.”, Nucl. Phys. B **212** (1983) 1.
- [20] R. Frezzotti *et al.* [Alpha Collaboration], “Lattice QCD with a chirally twisted mass term”, JHEP **0108** (2001) 058 [hep-lat/0101001].

- [21] R. Frezzotti and G. C. Rossi, “Chirally improving Wilson fermions. 1.  $O(a)$  improvement”, JHEP **0408** (2004) 007 [hep-lat/0306014].
- [22] A. Shindler, “Twisted mass lattice QCD”, Phys. Rept. **461** (2008) 37 [arXiv:0707.4093 [hep-lat]].
- [23] K. Jansen, C. Liu, M. Luscher, H. Simma, S. Sint, R. Sommer, P. Weisz and U. Wolff, “Nonperturbative renormalization of lattice QCD at all scales”, Phys. Lett. B **372** (1996) 275 [hep-lat/9512009].
- [24] J. Foley, K. Jimmy Juge, A. O’Cais, M. Peardon, S. M. Ryan and J. -I. Skullerud, “Practical all-to-all propagators for lattice QCD”, Comput. Phys. Commun. **172** (2005) 145 [hep-lat/0505023].
- [25] M. Foster *et al.* [UKQCD Collaboration], “Hadrons with a heavy color adjoint particle”, Phys. Rev. D **59** (1999) 094509 [hep-lat/9811010].
- [26] C. McNeile *et al.* [UKQCD Collaboration], “Decay width of light quark hybrid meson from the lattice”, Phys. Rev. D **73** (2006) 074506 [hep-lat/0603007].
- [27] S. Gusken, U. Low, K. H. Mutter, R. Sommer, A. Patel and K. Schilling, “Nonsinglet Axial Vector Couplings of the Baryon Octet in Lattice QCD”, Phys. Lett. B **227** (1989) 266.
- [28] M. Albanese *et al.* [APE Collaboration], “Glueball Masses and String Tension in Lattice QCD”, Phys. Lett. B **192** (1987) 163.
- [29] R. Frezzotti *et al.* [ETM Collaboration], “Electromagnetic form factor of the pion from twisted-mass lattice QCD at  $N_f = 2$ ”, Phys. Rev. D **79** (2009) 074506 [arXiv:0812.4042 [hep-lat]].
- [30] N. Carrasco *et al.* [ETM Collaboration], “Twisted Mass Lattice QCD,” PoS LATTICE **2012**, 105 (2012). [arXiv:1211.0565 [hep-lat]].
- [31] P. Lacock *et al.* [UKQCD Collaboration], “Orbitally excited and hybrid mesons from the lattice”, Phys. Rev. D **54** (1996) 6997 [hep-lat/9605025].
- [32] C. Michael, “Adjoint Sources in Lattice Gauge Theory”, Nucl. Phys. B **259** (1985) 58.
- [33] M. Luscher and U. Wolff, “How to Calculate the Elastic Scattering Matrix in Two-dimensional Quantum Field Theories by Numerical Simulation”, Nucl. Phys. B **339** (1990) 222.
- [34] B. Blossier, M. Della Morte, G. von Hippel, T. Mendes and R. Sommer, “On the generalized eigenvalue method for energies and matrix elements in lattice field theory”, JHEP **0904** (2009) 094 [arXiv:0902.1265 [hep-lat]].
- [35] A. K. Leibovich, Z. Ligeti, I. W. Stewart and M. B. Wise, “Semileptonic  $B$  decays to excited charmed mesons”, Phys. Rev. D **57** (1998) 308 [hep-ph/9705467].
- [36] B. Blossier *et al.* [ALPHA Collaboration], approximation,” JHEP **1012**, 039 (2010). [arXiv:1006.5816 [hep-lat]].
- [37] M. Wagner and M. Kalinowski, “Twisted mass lattice computation of charmed mesons with focus on  $D^{**}$ ”, arXiv:1310.5513 [hep-lat].
- [38] D. Spehler and S. F. Novaes, “Helicity wave functions for massless and massive spin-2 particles”, Phys. Rev. D **44** (1991) 3990.
- [39] S. Y. Choi, J. Lee, J. S. Shim and H. S. Song, “Spin-2 particle polarization”, J. Korean Phys. Soc. **25** (1992) 576.
- [40] S. Weinberg, “The Quantum theory of fields. Vol. 1: Foundations”, Cambridge, UK: Univ. Pr. (1995) 609 p